

<https://doi.org/10.3799/dqkx.2018.022>



# 漠河地区黑云母花岗闪长岩地球化学、Hf 同位素特征及其成因

李 良<sup>1</sup>, 孙丰月<sup>1\*</sup>, 李碧乐<sup>1</sup>, 陈广俊<sup>1</sup>, 许庆林<sup>2</sup>, 张雅静<sup>1</sup>, 钱 烨<sup>1</sup>, 王琳琳<sup>1</sup>

1. 吉林大学地球科学学院, 吉林长春 130061

2. 山东科技大学地球科学与工程学院, 山东青岛 266590

**摘要:**以往学者的研究多集中在印支期出露于漠河县城南的黑云母花岗闪长岩,而对该地区燕山早期构造演化的研究相对薄弱。运用 LA-ICP-MS 锆石 U-Pb 年代学、全岩地球化学与 Hf 同位素分析的方法确定其形成时代、岩浆源区性质及成岩构造背景。结果表明:该岩石的加权平均年龄分别为  $185 \pm 2$  Ma 和  $182 \pm 2$  Ma, 表明其形成于早侏罗世;岩石属于高钾钙碱性系列, A/CNK 介于  $0.90 \sim 1.03$ , Mg<sup>#</sup> 值为  $42 \sim 48$ , 具有高 Sr( $489 \times 10^{-6} \sim 653 \times 10^{-6}$ )低 Yb( $1.33 \times 10^{-6} \sim 1.99 \times 10^{-6}$ )的特征, 判定其属于埃达克岩类;岩石具有弧岩浆的微量元素特征, 轻重稀土元素分馏明显( $(La/Yb)_N = 8.36 \sim 15.6$ ), 较弱的 Eu 负异常( $Eu/Eu^* = 0.79 \sim 0.95$ ), 富集 Rb、K 等大离子亲石元素, 明显亏损 Nb、Ta、Ti 等高场强元素;岩石的  $\epsilon_{Hf}(t)$  值为  $-3.26 \sim -1.46$ , 二阶段模式年龄介于  $1.25 \sim 1.59$  Ga, 结合该时期的地幔特征认为该岩石岩浆起源于中元古代亏损地幔新增生的下地壳部分熔融。综合认为岩石形成于蒙古—鄂霍茨克洋板块向南俯冲的活动大陆边缘环境。

**关键词:**花岗闪长岩; 锆石 U-Pb 定年; Hf 同位素; 埃达克岩; 亏损地幔; 漠河地区; 地球化学; 地质年代学。

中图分类号: P581; P591.1

文章编号: 1000-2383(2018)02-0417-19

收稿日期: 2017-07-12

## Geochemistry, Hf Isotopes and Petrogenesis of Biotite Granodiorites in the Mohe Area

Li Liang<sup>1</sup>, Sun Fengyue<sup>1\*</sup>, Li Bile<sup>1</sup>, Chen Guangjun<sup>1</sup>, Xu Qinglin<sup>2</sup>, Zhang Yajing<sup>1</sup>, Qian Ye<sup>1</sup>, Wang Linlin<sup>1</sup>

1. College of Earth Sciences, Jilin University, Changchun 130061, China

2. College of Earth Science and Engineering, Shandong University of Science and Technology, Qingdao 266590, China

**Abstract:** Previous studies are mostly concentrated on the biotite granodiorites exposed during the Indosinian period in southern Mohe county, while the research on the Early Yanshanian tectonic evolution in this area is relatively weak. This paper presents new zircon U-Pb dating, Hf isotope, major and trace elements for biotite granodiorites in southern Mohe County for the discussion in their geochronology, magma sources and tectonic setting. Zircon dating results demonstrate that biotite granodiorites were formed in Early Jurassic ( $185 \pm 2$  Ma and  $182 \pm 2$  Ma). Geochemically, these rocks have  $A/CNK = 0.90 \sim 1.03$ ,  $Mg^{\#} = 42 \sim 48$ , belonging to the high-K calc-alkaline series. The pluton has features similar to adakitic rock with high Sr ( $489 \times 10^{-6} \sim 653 \times 10^{-6}$ ) and low Yb ( $1.33 \times 10^{-6} \sim 1.99 \times 10^{-6}$ ). They have the geochemistry of arc magmatic rocks, which are enriched LREE and LILE (e.g., Rb and K), depleted HREE and HFSE (e.g., Nb, Ta and Ti), as well as very weak negative Eu anomalies ( $Eu/Eu^* = 0.79 \sim 0.95$ ), indicating that the magma source was derived from the partial melting of lower crust. Zircon  $\epsilon_{Hf}(t)$  values and two-stage Hf model ages ( $t_{DM2}$ ) of do itite granodiorites range from  $-3.26$  to  $-1.46$  and  $1.25$  Ga to  $1.59$  Ga, respectively, indicative of formation from primary magmas generated by partial melting of thickened low crust that formed

基金项目:中国地质调查局项目(No.1212011085485);国家自然科学基金项目(No.41272093)。

作者简介:李良(1986—),男,博士研究生,主要从事矿床成矿理论与预测方面的研究。ORCID:0000-0002-0898-306X. E-mail:liliangjlu2011@163.com

\* 通讯作者:孙丰月,ORCID:0000-0001-9408-7298. E-mail:sunfeng0669@sina.com

引用格式:李良,孙丰月,李碧乐,等,2018.漠河地区黑云母花岗闪长岩地球化学、Hf 同位素特征及其成因.地球科学,43(2):417—435.

from the depleted mantle during the Meso- to Neoproterozoic. Considering the regional tectonic revolution, we suggest that the diotite granodiorite was formed in the setting of continuous southward subduction of Mongol-Okhotsk oceanic plate during the Early Mesozoic.

**Key words:** granodiorite; zircon U-Pb dating; Hf isotope; Adakite; depleted mantle; Mohe area; geochemistry; geochronology.

## 0 引言

埃达克岩是最先由 Defant and Drummond(1990)在研究阿留申群岛的埃达克岛新生代火山岩时引入地学界的一个岩石类型,指由俯冲洋壳在70~90 km 处发生部分熔融形成的与年轻( $\leqslant 25$  Ma)俯冲大洋岩石圈有关的新生代岛弧环境中的火山岩或侵入岩。该岩石具有以下特征(Defant and Drummond, 1990):  $\text{SiO}_2$  含量 $\geqslant 56\%$ 、 $\text{Al}_2\text{O}_3$  含量 $\geqslant 15\%$ (极少低于此值)、 $\text{MgO}$  含量 $<3\%$ (极少 $>6\%$ )、高 Sr(通常 $>400 \times 10^{-6}$ )、低 Y( $\leqslant 18 \times 10^{-6}$ ) 和 Yb( $\leqslant 1.9 \times 10^{-6}$ ) 含量,相对亏损重稀土元素(HREE)和高场强元素(HFSE),无 Eu 异常或微弱的正异常, $^{87}\text{Sr}/^{86}\text{Sr}$  通常 $<0.7040$ 。自 2000 年“埃达克岩”被引入国内以后,便引起了学术界的广泛关注(张旗等,2001,2004;王强等,2006;秦秀峰等,2007)。其中,张旗等(2001)发现中国东部的中生代火成岩具有“埃达克岩”的地球化学特征,但其形成与下地壳的部分熔融有关,而与俯冲洋壳无关,并由此提出了“C”型埃达克岩这一亚类。学者们(张旗等,2001; Xiao and Clemens, 2007; Ding et al., 2016)认为“C”型埃达克岩的形成与玄武岩浆底侵到加厚地壳( $>50$  km)底部导致下地壳部分熔融有关。随着研究的深入,埃达克岩的含义被不断扩展,许多埃达克岩具有不同的特征,来自不同的源岩、产于不同的环境、具有不同的成因,显示出多样性(张旗等,2004)。但对于扩展出来的“C”型埃达克岩则充满争议,争议的焦点集中在原始埃达克岩的定义能否扩展(翁望飞等,2011)。学者们对此众说纷坛(张旗等,2001,2004;王强等,2006;秦秀峰等,2007;翁望飞等,2011)。如今,埃达克岩一词已演变成具有某一类地球化学特征的岩石类型,其产出的构造背景已不仅仅局限于年轻洋壳俯冲带,该术语已不再具备成因和构造环境方面的意义(张旗等,2001,2004;翁望飞等,2011)。

研究表明,浅成低温热液 Au-Ag 及斑岩型 Cu-Cu-Au 矿床与埃达克岩具有密切的成因联系,该类岩石具有较强的成矿专属性,多数埃达克岩省也是重要的成矿省(Thieblemont et al., 1997; Sajona and Maury, 1998; Oyarzun et al., 2001; 张旗等,

2004)。Thieblemont et al.(1997)统计了全球 43 个 Au、Ag、Cu 和 Mo 低温热液和斑岩型矿床,发现其中 38 个与埃达克岩相关。Sajona and Maury(1998)发现菲律宾 14 个斑岩型铜矿和低温热液 Au 矿中有 12 个与埃达克岩有关。此外,我国的斑岩型铜(金、钼)矿大多与埃达克岩相关(张旗等,2004)。埃达克岩对该类矿床成矿作用的影响主要体现在:①在角闪岩相向榴辉岩相转变过程中角闪石发生分解、脱水并释放出大量流体,不仅有利于埃达克质岩浆的形成,还有利于 Au、Cu 等金属元素的萃取和迁移,产生的埃达克质岩浆成为潜在的富含挥发分的成矿母岩浆(Kay and Mpodozis, 2001; Rabbia et al., 2017);②板片熔融过程中带入大量的  $\text{Fe}_2\text{O}_3$  使熔体保持高氧逸度,有利于地幔中的亲硫元素 Cu、Au 等进入熔体并进行迁移(Oyarzun et al., 2001; 王强等,2006);而对 C 型埃达克岩来说,玄武质岩浆的底侵作用可以将大量 Au、Cu 从地幔带到下地壳底部而成为“矿源”,中国大多数金铜矿床与 C 型埃达克岩相关(张旗等,2009)。

研究区位于额尔古纳地块的北东端,兴—蒙造山带的东段,蒙古—鄂霍茨克缝合带的南侧。蒙古—鄂霍茨克造山带是一条具有较长地质历史的造山带,是古生代和早中生代造山作用形成的复合造山带(李锦铁等,2009; 许文良等,2013)。由于该造山带主要位于俄罗斯和蒙古境内,关于其对我国境内构造演化的影响的研究相对较少(许文良等,2013; Tang et al., 2014)。古生代和早中生代时期,蒙古—鄂霍茨克洋位于西伯利亚板块与华北板块之间,由于西伯利亚板块与华北板块独特的运动方式使得蒙古—鄂霍茨克洋的演化历史极为复杂(Zhao et al., 1990; Zorin, 1999; Parfenov et al., 2001; 李锦铁等,2004a)。蒙古—鄂霍茨克洋板块是否存在向南俯冲一直是学术界争论的焦点。但随着研究的深入,越来越多的资料显示蒙古—鄂霍茨克洋板块存在向南俯冲,发生了至少 4 期大规模岩浆事件(Wu et al., 2011; 许文良等,2013; Xu et al., 2013; Tang et al., 2014, 2016; Zhao et al., 2016)。额尔古纳地块北东端的漠河地区岩浆岩出露广泛、岩性多样,一直是探究蒙古—鄂霍茨克洋对我东北地区影响的热区,但以往学者的研究多集中在

印支期(Gou *et al.*, 2013; Tang *et al.*, 2014),燕山早期构造演化的研究则相对薄弱,且论及埃达克岩的文献较少(张炯飞等,2004;武广等,2008)。因此,本文选取研究程度相对较低的、出露于漠河县城南的具有埃达克岩特征的黑云母花岗闪长岩为研究对象,通过岩相学、锆石U-Pb年代学、地球化学及Hf同位素等分析方法,探讨其形成时代、岩石成因、岩浆源区性质和构造背景。

## 1 地质背景及样品描述

### 1.1 地质背景

额尔古纳地块位于西伯利亚板块东南缘(图1a),其构造—岩浆活动强烈,成矿条件优越,有众多金属矿床产出,如八大关斑岩型钼矿、砂宝斯金矿等。区域地层发育,主要为构成前寒武纪基底的中元古界兴华渡口群与新元古界浅变质岩系,古生界盖层为火山—碎屑岩和碳酸盐岩,中生界侏罗系、白垩系为火山—碎屑岩系及含煤沉积建造(内蒙古自治区地质矿产局,1991;黑龙江省地质矿产局,1993)。区内构造以断裂为主,以NE和近EW向为主;其中

NE向及其派生的NW向断裂主要受控于得尔布干深大断裂,而近EW向断裂的形成则与中生代蒙古—鄂霍茨克大洋闭合后的陆—陆碰撞造山过程有关(武广等,2007)。区域岩浆岩广泛发育,其中以古元古代(Wu *et al.*, 2012)和古生代中酸性侵入岩(Wu *et al.*, 2005; Zhao *et al.*, 2016)、中生代的侵入岩和火山岩(秦克章等,1999;王召林等,2010; Tang *et al.*, 2014, 2016; 李良等,2017)分布最为广泛,在漠河地区大面积出露并将基底熔蚀成孤岛状(图1b)。黑龙江省地质矿产局(1993)曾依据Sm-Nd法测得的漠河地区花岗岩年龄为638 Ma,将其划归为兴凯—萨拉伊尔期花岗岩,时代归属为新元古代。但越来越多的资料显示该花岗岩可能由各个时代的中酸性侵入岩组成(李锦轶等,2004b; 秦秀峰等,2007; Wu *et al.*, 2011)。中生代岩体沿蒙古—鄂霍茨克造山带两侧呈带状分布,大体呈NE向延伸,二者走向大体一致,其形成与蒙古—鄂霍茨克洋的演化息息相关(许文良等,2013; Xu *et al.*, 2013; Tang *et al.*, 2014, 2016)。

### 1.2 样品描述

本次样品采自漠河县城以南约30 km处的黑

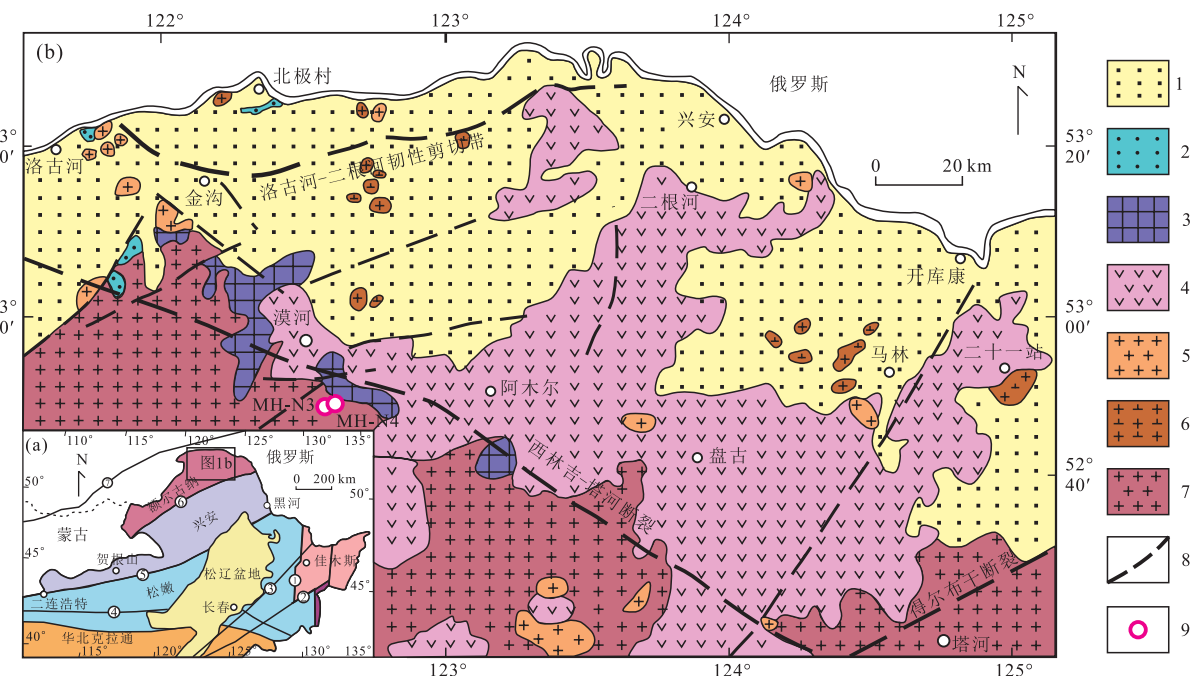


图1 中国东北地区构造分区图(a)和漠河地区地质简图(b)

Fig.1 Simplified geological map of NE China, showing the main tectonic subdivisions (a) and detailed geological map of the Mohe area, Heilongjiang province (b)

图a中主要断裂:①牡丹江断裂,②敦化—密山断裂,③伊通—伊兰断裂,④索伦—西拉木伦—长春断裂,⑤贺根山—黑河断裂,⑥喜桂图—塔源断裂,⑦蒙古—鄂霍茨克缝合带;图b:1.中生代沉积岩,2.古生代沉积岩,3.前寒武纪基底,4.中生代火山岩,5.中生代花岗岩,6.中生代花岗闪长岩,7.时代不明的花岗岩,8.主要断裂,9.采样地点;图a据Wu *et al.*(2007),图b据黑龙江省地质矿产局(1993)和李良等(2015)改编

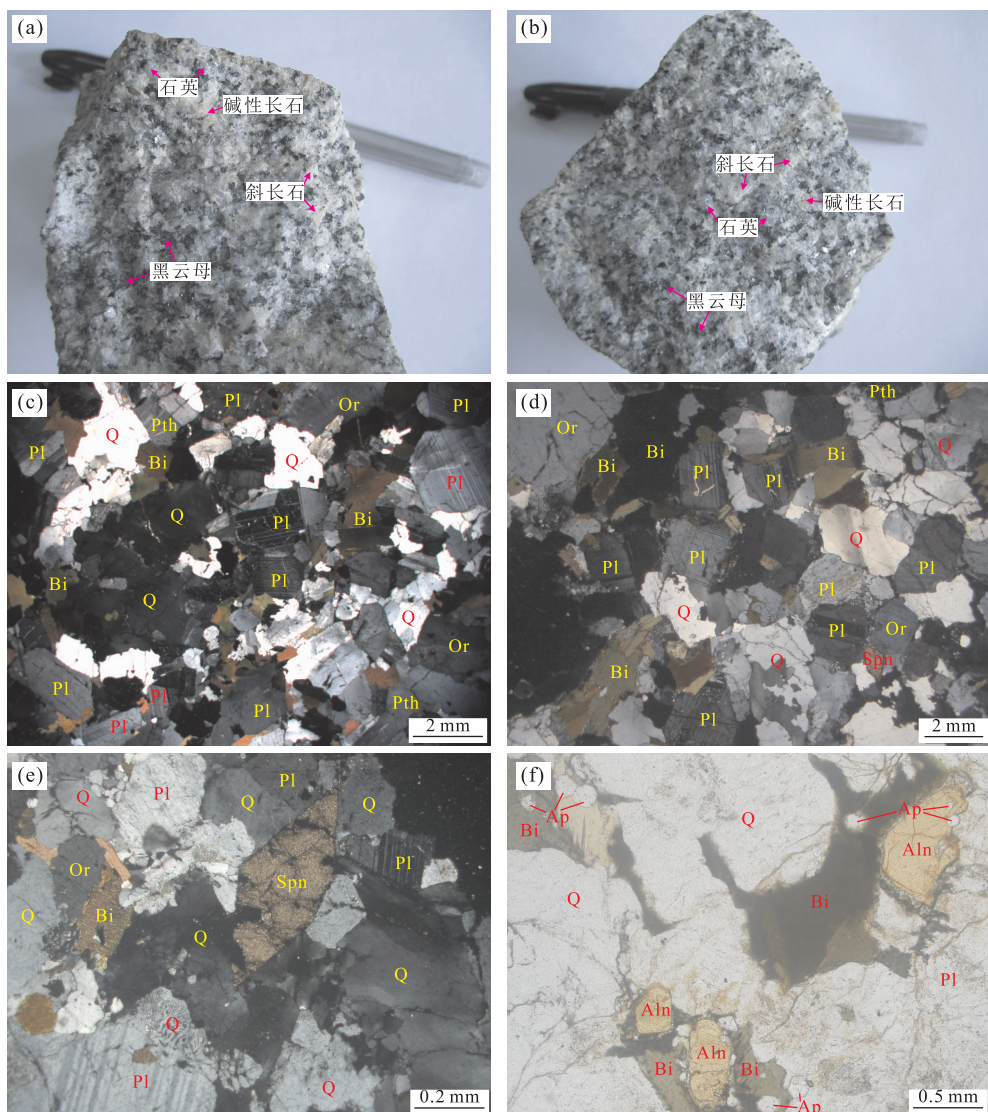


图 2 研究区黑云母花岗闪长岩手标本(a,b)和显微镜下照片(c~f)

Fig.2 Hand specimen photographs (a, b) and micrographs (c~f) of the biotite granodiorites in the study area  
 Aln.褐帘石; Ap.磷灰石; Bi.黑云母; Or.正长石; Pl.斜长石; Pth.条纹长石; Q.石英; Spn.榍石

云母花岗闪长岩体(图 1b),采样坐标分别为 52°49' 59"N、122°35'49"E, 52°50'05"N、122°35'58"E。岩体侵入到中元古代兴华渡口群片麻岩、片岩和斜长角闪岩中,呈侵入接触关系。岩石呈灰—灰黑色,发育花岗结构、块状构造(图 2a, 2b),主要由石英(~25%)、斜长石(~40%)、正长石(~15%)、条纹长石(~8%)、黑云母(~10%)和少量副矿物(~2%)组成(图 2c~2f)。石英呈他形—半自形粒状产出,粒度多为 0.5~1.5 mm,可见蠕虫结构。长石为半自形—自形板状,发育环带结构,粒度为 0.2~2.0 mm。黑云母以他形片状产于石英、长石颗粒之间,粒度为 0.2~1.5 mm。副矿物有榍石、磷灰石、褐帘石、锆石与磁铁矿等(图 3e, 3f)。

## 2 分析方法

### 2.1 LA-ICP-MS 锆石 U-Pb 定年

锆石挑选由河北省廊坊区域地质调查研究所实验室利用标准重矿物分离技术分选完成。经过双目镜下仔细挑选,将不同特征的锆石粘在双面胶上,并用无色透明的环氧树脂固定;待其固化之后,将表面抛光至锆石中心。在测试前,通过反射光和 CL 图像仔细研究锆石的晶体形态与内部结构特征,以选择最佳测试点。锆石制靶、反射光、阴极发光以及锆石 U-Pb 年龄测定和痕量元素分析均在西北大学大陆动力学国家重点实验室进行。本次测试采用的激光剥蚀束斑直径为 32  $\mu\text{m}$ , 激光剥蚀样品的深度为

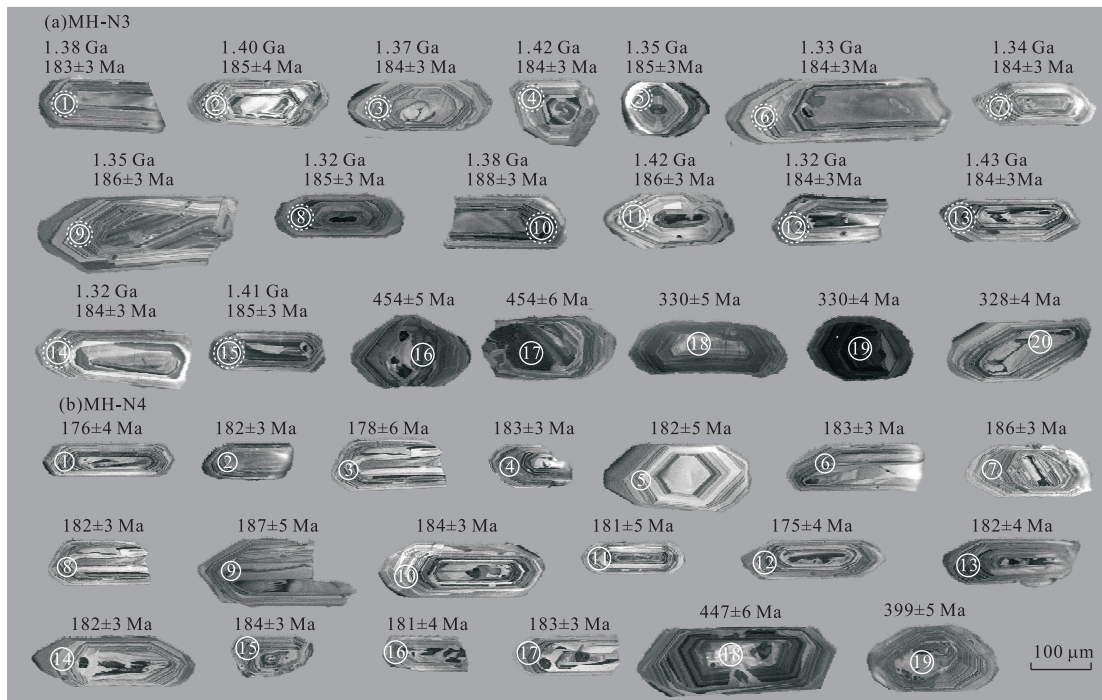


图3 黑云母花岗闪长岩部分锆石阴极发光图像

Fig.3 CL images of zircons selected for analysis from biotite granodiorites

实线圆圈代表U-Pb分析点,虚线圆圈代表相应的Hf同位素分析点;MH-N3样品的锆石图中第一排数值为二阶段模式年龄,第二排数值为锆石U-Pb表面年龄

20~40  $\mu\text{m}$ ;实验中采用He作为剥蚀物质的载气。锆石年龄采用国际标准锆石91500作为外标,元素含量采用NIST SRM610作为外标, $^{29}\text{Si}$ 作为内标元素(锆石中 $\text{SiO}_2$ 的质量分数为32.8%),分析方法见Yuan *et al.*(2004);普通铅校正采用Anderson(2002)推荐的方法;样品的同位素比值及元素含量计算采用ICPMsDataCal程序(Liu *et al.*, 2008, 2010),年龄计算及谐和图的绘制采用Isoplot程序(Ludwig, 2003)。

## 2.2 全岩化学分析

本次实验主量及微量元素的分析测试均在吉林大学测试科学实验中心完成。主量元素采用X射线荧光光谱仪(PW1401/10)测定(GB/T14506.28-93),相对标准偏差为2%~5%。微量元素和稀土元素分析采用美国安捷伦科技有限公司Agilent 7500A型耦合等离子体质谱仪测试(Z/T0223-2001),样品测试经国际标样BHVO-2、BC4-2和国家标样GBW07103、GB207104监控,微量元素和稀土元素的分析精度为:元素含量大于 $10 \times 10^{-6}$ 的误差小于5%,小于 $10 \times 10^{-6}$ 的误差小于10%。

## 2.3 Hf同位素分析

锆石Lu-Hf同位素测定在天津地质矿产研究所

同位素实验的LA-MC-ICP-MS仪器上完成,实验中使用的多接收器电感耦合等离子体质谱仪为美国Thermo Fisher公司生产的NEPTUNE,分析方法的详细流程见耿建珍等(2011)。采用 $^{179}\text{Hf}/^{177}\text{Hf} = 0.7325$ (Patchett *et al.*, 1980)、 $^{173}\text{Yb}/^{172}\text{Yb} = 1.35274$ (Chu *et al.*, 2002)对Hf、Yb同位素比值进行指数归一化质量歧视矫正。 $^{176}\text{Hf}$ 同质异位素干扰校正公式见Chu *et al.*(2002), $^{176}\text{Yb}/^{172}\text{Yb} = 0.5887$ , $^{175}\text{Lu}/^{176}\text{Lu} = 0.02655$ (Chu *et al.*, 2002)。 $\omega(^{176}\text{Hf})/\omega(^{177}\text{Hf})$ 比值(0.282772)及 $\omega(^{176}\text{Lu})/\omega(^{177}\text{Hf})$ 比值(0.0332),Hf模式年龄计算使用当前亏损地幔的 $\omega(^{176}\text{Hf})/\omega(^{177}\text{Hf})$ 比值(0.28325)和 $\omega(^{176}\text{Lu})/\omega(^{177}\text{Hf})$ 比值(0.0150)(Griffin *et al.*, 2002)。

## 3 分析结果

### 3.1 LA-ICP-MS锆石年代学

样品MH-N3的锆石粒度为 $120\sim350\mu\text{m}$ ,具有完整的晶形、均匀的内部结构和清晰的振荡环带(图3),大多数锆石的Th/U值 $\geq 0.4$ ,显示为岩浆成因的锆石。对于Th/U值为0.08的锆石,可能为受到后期热扰动所致。如表1所示,15粒锆石的

表 1 漠河县城南黑云母花岗闪长岩锆石 LA-ICP-MS U-Pb 同位素分析结果

Table 1 Zircon LA-ICP-MS U-Pb dating results for biotite granodiorites in southern Mohe county

分析点	含量( $10^{-6}$ )		同位素比值						同位素年龄(Ma)											
	Pb	Th	Th/U	$^{207}\text{Pb}/^{206}\text{Pb}$	$1\sigma$	$^{207}\text{Pb}/^{235}\text{U}$	$1\sigma$	$^{208}\text{Pb}/^{238}\text{U}$	$1\sigma$	$^{207}\text{Pb}/^{232}\text{Th}$	$1\sigma$	$^{207}\text{Pb}/^{206}\text{Pb}$	$1\sigma$	$^{207}\text{Pb}/^{235}\text{U}$	$1\sigma$	$^{206}\text{Pb}/^{238}\text{U}$	$1\sigma$	$^{208}\text{Pb}/^{232}\text{Th}$	$1\sigma$	
MH-N3-01	17.3	406	473	0.86	0.0524	0.00023	0.2077	0.0071	0.0288	0.0004	0.0089	0.0002	301	52	192	6	183	3	180	3
MH-N3-02	9.32	67.4	262	0.26	0.0540	0.00039	0.2165	0.0142	0.0291	0.0006	0.0105	0.0006	370	112	199	12	185	4	210	11
MH-N3-03	12.5	176	372	0.47	0.0509	0.00024	0.2030	0.0092	0.0289	0.0004	0.0091	0.0001	237	111	188	8	184	3	183	2
MH-N3-04	10.7	177	304	0.58	0.0501	0.00024	0.2002	0.0075	0.0290	0.0004	0.0084	0.0002	199	60	185	6	184	3	169	3
MH-N3-05	22.6	49.5	595	0.08	0.0499	0.00019	0.1998	0.0069	0.0290	0.0004	0.0092	0.0001	190	88	185	6	185	3	184	2
MH-N3-06	9.23	77	269	0.29	0.0513	0.00026	0.2046	0.0084	0.0289	0.0004	0.0105	0.0003	256	66	189	7	184	3	211	6
MH-N3-07	8.96	78.1	225	0.35	0.0520	0.00028	0.2075	0.0095	0.0289	0.0005	0.0097	0.0003	287	76	191	8	184	3	196	6
MH-N3-08	7.52	93.8	220	0.43	0.0538	0.00027	0.2159	0.0090	0.0291	0.0004	0.0103	0.0003	363	66	199	7	185	3	207	5
MH-N3-09	12.7	95.2	356	0.27	0.0508	0.00027	0.2047	0.0092	0.0292	0.0005	0.0099	0.0003	231	75	189	8	186	3	199	6
MH-N3-10	12.8	125	369	0.34	0.0519	0.00028	0.2115	0.0096	0.0296	0.0005	0.0089	0.0003	279	74	195	8	188	3	179	5
MH-N3-11	16.7	370	459	0.81	0.0503	0.00020	0.2029	0.0057	0.0293	0.0004	0.0086	0.0001	209	40	188	5	186	3	172	3
MH-N3-12	8.73	68.8	270	0.25	0.0533	0.00029	0.2131	0.0098	0.0290	0.0005	0.0092	0.0003	342	74	196	8	184	3	185	6
MH-N3-13	14.7	252	430	0.59	0.0513	0.00024	0.2038	0.0074	0.0289	0.0004	0.0091	0.0002	245	56	188	6	184	3	184	4
MH-N3-14	18.7	207	525	0.39	0.0532	0.00023	0.2121	0.0068	0.0289	0.0004	0.0093	0.0002	337	47	195	6	184	3	188	4
MH-N3-15	16.4	248	432	0.57	0.0516	0.00031	0.2075	0.0121	0.0292	0.0005	0.0092	0.0001	268	141	191	10	185	3	185	2
MH-N3-16	96.4	643	1144	0.56	0.0576	0.00018	0.5795	0.0085	0.0729	0.0009	0.0205	0.0002	516	15	464	5	454	5	410	5
MH-N3-17	51.5	146	630	0.23	0.0631	0.00021	0.6349	0.0116	0.0730	0.0010	0.0314	0.0005	710	19	499	7	454	6	625	9
MH-N3-18	8.96	78.1	225	0.35	0.0558	0.00022	0.4036	0.0115	0.0525	0.0007	0.0258	0.0007	443	39	344	8	330	5	515	13
MH-N3-19	39.7	173	725	0.24	0.0580	0.00021	0.4202	0.0095	0.0525	0.0007	0.0219	0.0004	530	27	356	7	330	4	437	8
MH-N3-20	24.5	205	442	0.46	0.0572	0.00021	0.4120	0.0098	0.0522	0.0007	0.0122	0.0002	500	30	350	7	328	4	245	4
MH-N4-01	10.2	55.5	291	0.19	0.0518	0.00029	0.1973	0.0100	0.0276	0.0006	0.0103	0.0004	275	79	183	8	176	4	206	9
MH-N4-02	7.61	47.5	213	0.22	0.0502	0.00024	0.1985	0.0079	0.0287	0.0005	0.0089	0.0003	204	59	184	7	182	3	179	6
MH-N4-03	15.7	312	449	0.70	0.0520	0.00061	0.2006	0.0225	0.0280	0.0009	0.0079	0.0005	286	194	186	19	178	6	159	11
MH-N4-04	11.4	166	311	0.53	0.0506	0.00021	0.2011	0.0067	0.0289	0.0005	0.0089	0.0002	220	45	186	6	183	3	179	4
MH-N4-05	10.2	152	281	0.54	0.0545	0.00047	0.2150	0.0176	0.0286	0.0007	0.0092	0.0005	390	138	198	15	182	5	185	10
MH-N4-06	11	158	305	0.52	0.0510	0.00023	0.2028	0.0074	0.0288	0.0005	0.0078	0.0002	240	51	187	6	183	3	158	4
MH-N4-07	15.8	48.3	470	0.10	0.0522	0.00021	0.2105	0.0065	0.0292	0.0005	0.0129	0.0005	286	39	194	5	186	3	258	9
MH-N4-08	11.8	166	330	0.50	0.0498	0.00021	0.1969	0.0065	0.0287	0.0005	0.0086	0.0002	186	45	183	6	182	3	173	4
MH-N4-09	11.3	154	269	0.57	0.0557	0.00048	0.2258	0.0181	0.0294	0.0008	0.0095	0.0005	440	133	207	15	187	5	192	9
MH-N4-10	10.1	127	282	0.45	0.0515	0.00025	0.2058	0.0086	0.0290	0.0005	0.0084	0.0002	264	62	190	7	184	3	168	5
MH-N4-11	8.04	124	193	0.64	0.0506	0.00057	0.1982	0.0213	0.0284	0.0009	0.0093	0.0005	223	186	184	18	181	5	187	10
MH-N4-12	14.6	366	360	1.02	0.0500	0.00048	0.1897	0.0178	0.0275	0.0006	0.0087	0.0001	197	219	176	15	175	4	175	3
MH-N4-13	11.9	177	323	0.55	0.0553	0.00031	0.2188	0.0106	0.0287	0.0006	0.0092	0.0003	424	73	201	9	182	4	186	5
MH-N4-14	29.7	915	704	1.30	0.0515	0.00021	0.2033	0.0063	0.0286	0.0005	0.0083	0.0001	262	40	188	5	182	3	167	3
MH-N4-15	19.8	381	519	0.73	0.0521	0.00025	0.2078	0.0082	0.0289	0.0005	0.0093	0.0002	289	56	192	7	184	3	188	4
MH-N4-16	13.9	154	394	0.39	0.0547	0.00044	0.2150	0.0161	0.0285	0.0007	0.0118	0.0001	400	125	198	13	181	4	238	13
MH-N4-17	12.4	32	371	0.09	0.0514	0.00023	0.2042	0.0074	0.0288	0.0005	0.0118	0.0005	258	51	189	6	183	3	237	10
MH-N4-18	58.5	193	843	0.23	0.0606	0.00023	0.5596	0.0149	0.0717	0.0010	0.0189	0.0004	625	31	477	9	447	6	378	8
MH-N4-19	55.9	97.8	841	0.12	0.0549	0.00018	0.4836	0.0081	0.0639	0.0008	0.0220	0.0004	406	18	401	6	399	5	440	8

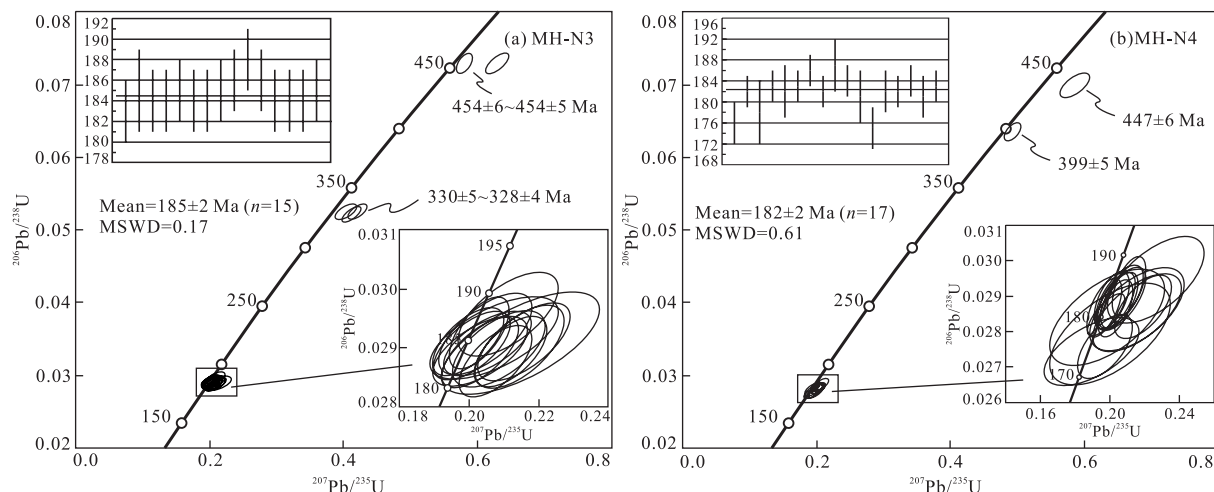
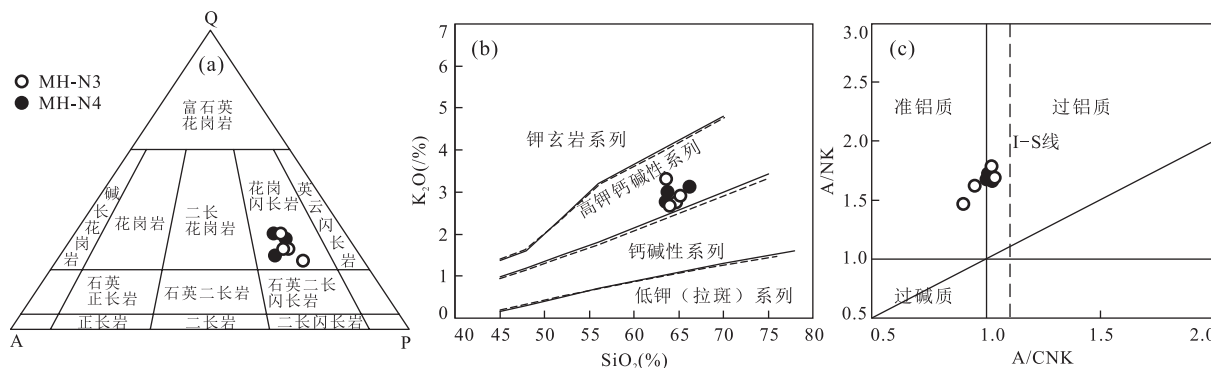


图4 漠河县城南黑云母花岗闪长岩样品锆石U-Pb年龄谐和图

Fig.4 Zircon U-Pb concordia diagrams for biotite granodiorites in southern Mohe county

图5 黑云母花岗闪长岩QAP图解(a)、SiO<sub>2</sub>-K<sub>2</sub>O图解(b)和A/CNK-A/NK图解(c)Fig.5 QAP (a), SiO<sub>2</sub> vs. K<sub>2</sub>O (b) and A/CNK vs. A/NK (c) diagrams of biotite granodiorites

图a底图据 Streckeisen(1976);图b底图据 Peccerillo and Taylor(1976);图c底图据 Maniar and Piccoli(1989)

<sup>206</sup>Pb/<sup>238</sup>U年龄为183±3~188±3 Ma,所有数据均落在谐和线上或附近,加权平均年龄为185±2 Ma (MSWD=0.17)(图4a),代表了岩浆的冷却结晶年龄。此外,样品存在少量晚奥陶世(454 Ma)和早石炭世(330~328 Ma)的继承锆石(图3)。

样品MH-N4锆石的粒度为100~300 μm,具有完整的晶形、均匀的内部结构和清晰的振荡环带(图3),大多数锆石的Th/U值≥0.4,为岩浆成因的锆石。对于Th/U值为0.09的锆石,可能为受到后期热扰动所致。如表1所示,17粒锆石的<sup>206</sup>Pb/<sup>238</sup>U年龄为175±4~187±5 Ma,所有数据均落在谐和线上或附近,加权平均年龄为182±2 Ma (MSWD=0.61)(图4b),代表了岩浆的冷却结晶年龄,表明该岩石形成于早侏罗世。此外,样品存在少量晚奥陶世(447 Ma)和早泥盆世(399 Ma)的继承锆石(图3)。

### 3.2 地球化学特征

如表2所示,样品MH-N3与MH-N4具有基本一致的地球化学特征,岩石具有富硅(SiO<sub>2</sub>含量为63.56%~66.32%)、富铝(Al<sub>2</sub>O<sub>3</sub>含量为16.58%~17.34%)、低磷(P<sub>2</sub>O<sub>5</sub>含量为0.17%~0.23%)和低钛(TiO<sub>2</sub>含量为0.55%~0.80%)的特征。岩石全碱含量较高(6.67%~8.79%),Na<sub>2</sub>O/K<sub>2</sub>O比值为1.29~1.64,MgO含量与Mg<sup>#</sup>值(Mg<sup>#</sup>=100×Mg<sup>2+</sup>/(Mg<sup>2+</sup>+TFe<sup>2+</sup>))分别为1.22%~1.98%与42~48.QAP图解中样品落入花岗闪长岩区域(图5a);在SiO<sub>2</sub>-K<sub>2</sub>O图解中样品属于高钾钙碱性系列(图5b);铝过饱和指数(A/CNK)介于0.90~1.03之间,样品主要落入准铝质范围,属于I型花岗岩(图5c)。

黑云母花岗闪长岩样品的球粒陨石标准化稀土元素配分曲线同样显示右倾模式(图6a),稀土元素

表 2 漠河县城南黑云母花岗闪长岩主量(%)、微量元素( $10^{-6}$ )分析结果Table 2 Major elements (%) and trace elements ( $10^{-6}$ ) compositions for biotite granodiorites in southern Mohe county

样品号	MH-N3-B1	MH-N3-B2	MH-N3-B3	MH-N3-B4	MH-N4-B1	MH-N4-B2	MH-N4-B3
SiO <sub>2</sub>	65.00	64.38	64.56	63.56	63.82	63.90	66.32
TiO <sub>2</sub>	0.73	0.66	0.64	0.55	0.80	0.76	0.63
Al <sub>2</sub> O <sub>3</sub>	16.82	16.58	16.96	16.76	17.10	17.34	16.63
FeO <sup>T</sup>	3.90	4.05	4.11	3.87	3.75	3.53	2.96
MnO	0.06	0.12	0.10	0.10	0.05	0.04	0.04
MgO	1.98	1.70	1.81	1.96	1.58	1.54	1.22
CaO	3.54	3.97	3.89	3.95	3.80	3.93	3.35
Na <sub>2</sub> O	4.13	4.40	3.96	4.68	4.15	4.29	4.02
K <sub>2</sub> O	2.89	2.68	2.71	3.39	2.98	2.74	3.13
P <sub>2</sub> O <sub>5</sub>	0.21	0.21	0.23	0.18	0.22	0.21	0.17
LOI	0.53	0.55	0.30	0.22	0.43	0.44	0.39
Total	99.91	99.40	99.40	99.40	99.28	99.27	99.34
ALK	7.02	7.08	6.67	8.07	7.14	7.03	7.15
Na <sub>2</sub> O/K <sub>2</sub> O	1.43	1.64	1.46	1.38	1.39	1.57	1.29
A/CNK	1.03	0.96	1.03	0.90	1.01	1.01	1.03
Mg <sup>#</sup>	48	43	44	47	43	44	42
La	17.5	19.2	27.1	15.5	41.0	38.2	25.4
Ce	46.6	53.0	61.2	41.8	83.7	75.6	62.4
Pr	5.71	5.84	7.07	4.74	10.8	9.74	7.98
Nd	24.9	25.3	30.4	21.0	39.7	36.3	30.7
Sm	4.50	4.60	5.42	3.95	6.55	6.13	5.92
Eu	1.16	1.23	1.39	0.96	1.81	1.67	1.43
Gd	3.48	3.58	4.28	3.41	5.20	4.92	5.13
Tb	0.45	0.45	0.54	0.47	0.66	0.62	0.71
Dy	2.49	2.40	2.80	2.70	3.25	3.11	3.85
Ho	0.45	0.43	0.49	0.48	0.65	0.59	0.75
Er	1.37	1.29	1.51	1.47	1.82	1.67	2.10
Tm	0.20	0.19	0.23	0.21	0.28	0.26	0.30
Yb	1.39	1.35	1.58	1.33	1.99	1.76	1.83
Lu	0.20	0.21	0.24	0.19	0.31	0.29	0.27
ΣREE	111	119	144	98.1	198	181	149
HREE	10.0	9.89	11.7	10.3	14.2	13.2	14.9
(La/Yb) <sub>N</sub>	9.08	10.2	12.3	8.36	14.8	15.6	10.0
Eu/Eu <sup>*</sup>	0.90	0.92	0.88	0.80	0.95	0.93	0.79
V	82.3	76.9	81.5	58.9	85.0	79.0	69.0
Cr	6.24	7.63	9.01	7.06	6.56	8.34	7.83
Co	8.15	7.88	8.70	6.51	6.87	6.65	8.22
Ni	7.00	6.16	6.08	4.89	6.52	5.37	6.21
Sn	2.64	2.51	2.69	2.76	3.00	3.00	3.00
Cs	2.88	2.45	2.42	3.22	3.00	2.74	4.11
Rb	47.0	41.4	50.0	59.3	114	100	118
Sr	541	504	563	489	653	622	587
Y	11.3	12.6	15.3	11.9	19.4	17.3	21.7
Ba	649	604	620	614	987	823	943
Zr	204	88.2	261	43.9	250	220	210
Nb	12.8	12.1	13.1	12.2	16.5	14.5	15.1
Hf	3.52	1.81	4.53	1.03	6.60	6.10	5.30
Ta	0.94	0.92	1.01	0.94	1.50	1.40	1.40
Ga	28.2	26.5	27.8	26.4	27.9	26.3	26.4
Pb	14.4	14.2	14.8	15.4	18.6	17.3	20.7
Th	5.26	4.84	6.24	4.60	8.77	8.46	8.24
U	2.01	1.97	2.25	1.92	2.59	2.17	2.03

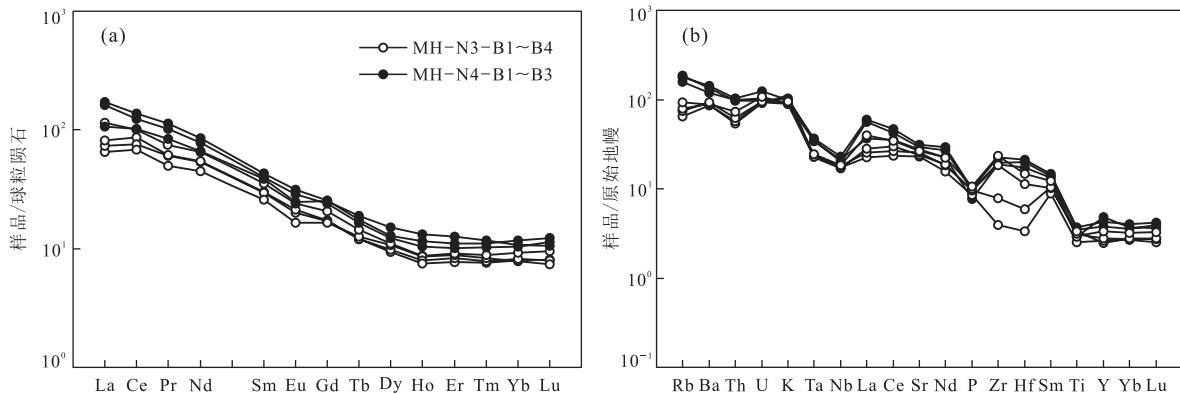


图6 黑云母花岗闪长岩稀土元素球粒陨石标准化配分图(a)和微量元素原始地幔标准化蛛网图(b)

Fig.6 Chondrite-normalized REE patterns (a) and primitive mantle-normalized trace element spider diagrams (b) for biotite granodiorites

图a底图据 Boynton (1984);图b底图据 Sun and McDonough (1989)

表3 漠河县城南黑云母花岗闪长岩锆石Hf同位素分析结果

Table 3 Zircon Lu-Hf isotopic data for biotite granodiorites in southern Mohe county

分析点	<i>t</i> (Ma)	$^{176}\text{Yb}/^{177}\text{Hf}$	$2\sigma$	$^{176}\text{Lu}/^{177}\text{Hf}$	$2\sigma$	$^{176}\text{Hf}/^{177}\text{Hf}$	$2\sigma$	$\epsilon_{\text{Hf}}(0)$	$\epsilon_{\text{Hf}}(t)$	$2\sigma$	$t_{\text{DM1}}(\text{Hf})$	$t_{\text{DM2}}(\text{Hf})$	$f_{\text{Lu/Hf}}$
MH-N3-1	183	0.019 292	0.000 218	0.000 582	0.000 004	0.282 592	0.000 014	-6.36	-2.41	0.50	924	1 378	-0.98
MH-N3-2	185	0.013 751	0.000 062	0.000 434	0.000 002	0.282 582	0.000 014	-6.71	-2.70	0.49	934	1 398	-0.99
MH-N3-3	184	0.025 231	0.000 089	0.000 723	0.000 001	0.282 595	0.000 015	-6.26	-2.31	0.53	923	1 372	-0.98
MH-N3-4	184	0.011 502	0.000 151	0.000 376	0.000 003	0.282 574	0.000 015	-6.98	-2.99	0.52	943	1 416	-0.99
MH-N3-5	185	0.014 551	0.000 385	0.000 452	0.000 010	0.282 605	0.000 015	-5.92	-1.91	0.53	903	1 348	-0.99
MH-N3-6	184	0.022 926	0.000 311	0.000 697	0.000 013	0.282 613	0.000 016	-5.61	-1.65	0.56	897	1 331	-0.98
MH-N3-7	184	0.042 380	0.001 638	0.001 156	0.000 044	0.282 610	0.000 018	-5.74	-1.85	0.63	913	1 343	-0.97
MH-N3-8	185	0.028 355	0.000 905	0.000 768	0.000 021	0.282 618	0.000 018	-5.43	-1.46	0.63	891	1 319	-0.98
MH-N3-9	186	0.057 628	0.000 663	0.001 457	0.000 022	0.282 607	0.000 018	-5.85	-1.94	0.63	925	1 351	-0.96
MH-N3-10	188	0.025 143	0.000 246	0.000 757	0.000 008	0.282 592	0.000 013	-6.35	-2.32	0.46	928	1 376	-0.98
MH-N3-11	186	0.013 000	0.000 183	0.000 391	0.000 002	0.282 571	0.000 015	-7.12	-3.09	0.52	949	1 423	-0.99
MH-N3-12	184	0.022 687	0.000 141	0.000 679	0.000 004	0.282 617	0.000 017	-5.49	-1.53	0.60	892	1 323	-0.98
MH-N3-13	184	0.007 467	0.000 080	0.000 283	0.000 001	0.282 567	0.000 015	-7.26	-3.26	0.54	952	1 433	-0.99
MH-N3-14	184	0.020 418	0.000 221	0.000 590	0.000 005	0.282 617	0.000 016	-5.49	-1.52	0.57	889	1 322	-0.98
MH-N3-15	185	0.016 438	0.000 132	0.000 493	0.000 004	0.282 577	0.000 017	-6.88	-2.88	0.60	942	1 410	-0.99

总量较高( $\Sigma\text{REE}=98.1 \times 10^{-6} \sim 198 \times 10^{-6}$ ),轻重稀土分馏明显( $(\text{La/Yb})_N=8.36 \sim 15.6$ ),富集轻稀土元素,具有微弱的Eu负异常( $\text{Eu/Eu}^*=0.79 \sim 0.95$ ).原始地幔标准化微量元素蛛网图显示,岩石富集Ba,K等大离子亲石元素,明显亏损Nb,Ta,Ti和Th等高场强元素(图6b).

### 3.3 Hf同位素

选择样品MH-N3的锆石进行Hf同位素分析,结果列于表3中.岩石的15个分析点的 $^{176}\text{Hf}/^{177}\text{Hf}$ 值分布于0.282 567~0.282 618之间, $\epsilon_{\text{Hf}}(t)$ 值为-3.26~-1.46,二阶段Hf模式年龄为1.25~1.59 Ga,平均为1.37 Ga,落入中亚造山带东段火成岩Hf同位素组成的区域(Yang *et al.*, 2006),与额尔古纳地块早中生代花岗质岩石的Hf同位素组成基本一致(图7).

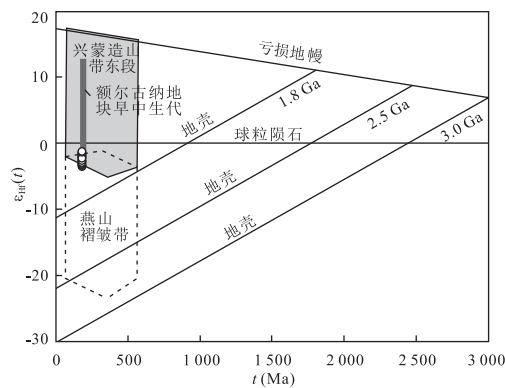


图7 黑云母花岗闪长岩锆石Hf同位素特征

Fig.7 Hf isotopic compositions of zircons from biotite granodiorites

兴蒙造山带东段与燕山褶皱带Hf同位素组成引自 Yang *et al.* (2006);额尔古纳地块早中生代花岗质岩石的Hf同位素组成引自 Tang *et al.* (2016)

## 4 讨论

### 4.1 岩石成因与岩浆源区性质

黑云母花岗闪长岩具有埃达克岩的特征:Sr 含量为  $489 \times 10^{-6} \sim 653 \times 10^{-6}$ (平均为  $566 \times 10^{-6}$ )、Yb 含量为  $1.33 \times 10^{-6} \sim 1.99 \times 10^{-6}$ (平均为  $1.60 \times 10^{-6}$ )、Y 含量为  $11.3 \times 10^{-6} \sim 21.7 \times 10^{-6}$ (平均为  $15.6 \times 10^{-6}$ )及微弱的负 Eu 异常( $\text{Eu}/\text{Eu}^* = 0.79 \sim 0.90$ ). 在图 8 中, 样品均落入埃达克岩的区域, 同时岩石具有富 K( $\text{K}_2\text{O}/\text{Na}_2\text{O} = 0.61 \sim 0.78$ ) 和贫 Mg( $\text{Mg}^\# = 42 \sim 48$ )、Cr( $6.24 \times 10^{-6} \sim 9.01 \times 10^{-6}$ )、Ni( $4.89 \times 10^{-6} \sim 7.00 \times 10^{-6}$ ) 的特征, 属于高钾钙碱性系列, 应为高钾钙碱性埃达克岩(张旗等, 2004). 目前, 埃达克质岩石的成因概括起来主要有以下几种:(1)俯冲洋壳的部分熔融(即 O型, 原始定义; Defant and Drummond, 1990);(2)加厚玄武质下地壳部分熔融(即 C型; Atherton and Petford, 1993; Castillo *et al.*, 1999; 张旗等, 2001; Lai *et al.*, 2003; Wang *et al.*, 2003a, 2003b);(3)拆沉下地壳的部分熔融(Gao *et al.*, 2004);(4)结晶分异作用影响(Macpherson *et al.*, 2006);(5)岩浆混合作用(Xiong *et al.*, 2003).

通常认为,O型埃达克岩具有富钠贫钾的特征( $\text{Na}_2\text{O}/\text{K}_2\text{O} > 2$ ), 同时具有高的 Sr/Y 值(>40)和低的 Yb 含量( $\text{Yb} < 1.9 \times 10^{-6}$ )(Defant and Drummond, 1990; Stern and Kilian, 1996), 而 C型埃达克岩相对于 O型明显富钾( $\text{Na}_2\text{O}/\text{K}_2\text{O} \geq 1$ ; 张旗等, 2001). 但是, 该花岗闪长岩的重稀土含量偏高(HREE =  $9.89 \times 10^{-6} \sim 14.9 \times 10^{-6}$ )、 $(\text{La}/\text{Yb})_N$  值较低( $8.36 \sim 15.6$ )、 $\text{Na}_2\text{O}/\text{K}_2\text{O}$  值偏低( $1.29 \sim 1.64$ ), 与俯冲洋壳部分熔融形成的埃达克岩有本质区别(Defant and Drummond, 1990). 拆沉下地壳熔融的埃达克质岩石通常形成于伸展构造背景(Wang *et al.*, 2003a, 2003b; Xiong *et al.*, 2005), 而该时期漠河地区显然不具备这样的构造环境(Tomurtogoo *et al.*, 2005; Orolmaa *et al.*, 2008; Chen *et al.*, 2011; 许文良等, 2013; Tang *et al.*, 2014, 2016). 研究区中生代发生地壳拆沉作用的时间在中一晚侏罗世(韦忠良等, 2008; 孟恩等, 2011; Xu *et al.*, 2013), 该时期的岩浆岩与早侏罗世黑云母花岗闪长岩的地球化学特征也存在显著的差别(Zhang *et al.*, 2008; 孟恩等, 2011; Xu *et al.*, 2013). 岩石中同样未发现可能与拆沉作用有关的榴辉岩捕虏体或者基性的残余体(高山和金振民, 1997). 岩石 MREE 和 HREE

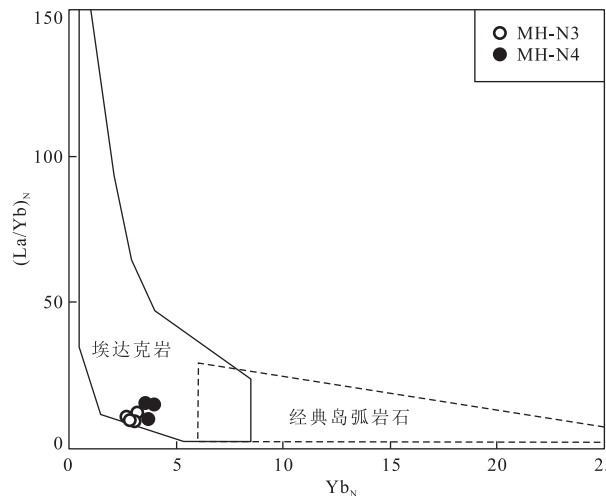


图 8 黑云母花岗闪长岩  $\text{Yb}_N$ - $(\text{La}/\text{Yb})_N$  判别图解

Fig.8  $\text{Yb}_N$  vs.  $(\text{La}/\text{Yb})_N$  diagram for biotite granodiorites  
底图据 Defant and Drummond (1990)

之间不是以上凹曲线模式分布(图 6a),  $\text{Eu}/\text{Eu}^*$  值为  $0.79 \sim 0.95$ , 而且  $(\text{Dy}/\text{Yb})_N$  值和  $\text{SiO}_2$  之间不存在明显的负相关性, 表明结晶分异过程不是控制岩浆演化的主要途径(Macpherson *et al.*, 2006; 王强等, 2006; 刘金龙等, 2015a, 2016). 锆石 Hf 同位素变化范围较小的  $\epsilon_{\text{Hf}}(t)$  值( $-3.26 \sim -1.46$ )表明其并没有发生岩浆混合作用. 因此, 该埃达克质岩石的形成可能与增厚的下地壳部分熔融有关(刘金龙等, 2015a, 2016; 侯红星等, 2016).

研究结果表明, 洋中脊玄武岩部分熔融只产生  $\text{Mg}^\# < 45$  的熔体, 但熔体只要与橄榄岩发生 10% 的混染便可使熔体的  $\text{Mg}^\#$  值从 45 上升至 55(Rapp and Watson, 1995), 而典型埃达克岩的  $\text{Mg}^\#$  值在 50 左右(Martin, 1999; Richards and Kerrich, 2007). 该花岗闪长岩样品的  $\text{Mg}^\#$  值为  $42 \sim 48$ , 只有 2 个分析点大于 45, 反映其岩浆源区受到橄榄岩混染的程度很低. 在图 9 中样品基本落入“与加厚下地壳相关的埃达克岩”区域, 而与“与俯冲洋壳相关的埃达克岩”的特征差异明显, 结合  $\text{Na}_2\text{O}/\text{K}_2\text{O}$  值、Sr/Y 值和 HREE 等特征笔者认为该埃达克岩的岩浆应来源于下地壳的部分熔融. 同时, 该岩石属于 I 型花岗岩, 相关的源区判别图解显示其原始岩浆来源于角闪岩的部分熔融(图 10). 综上可知, 该花岗闪长岩的岩浆应起源于加厚下地壳铁镁质岩石的部分熔融.

岩石富硅、富钾、贫镁, 属于高钾钙碱性系列, 富集 LILEs 和 LREE、亏损 HFSEs 等特征反映其为壳源成因(Mckenzie, 1989). 岩石无明显的 Eu 异常

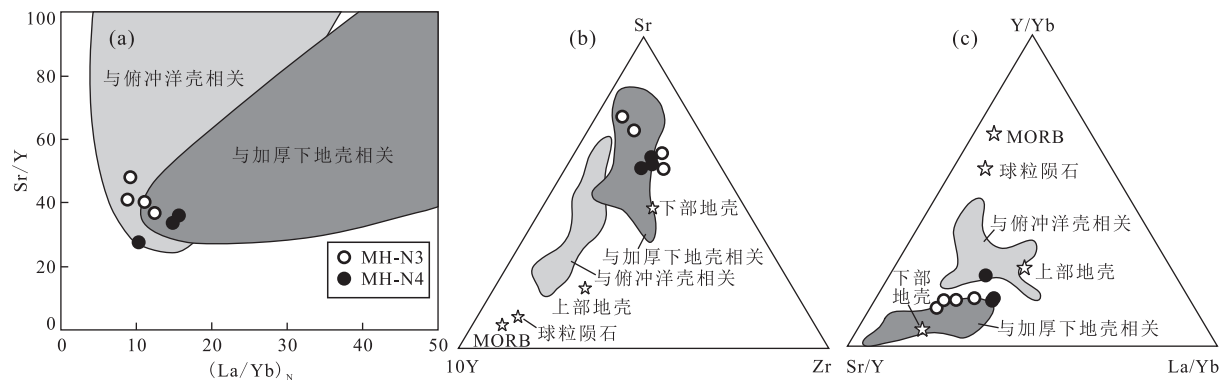
图9 黑云母花岗闪长岩 Sr/Y-(La/Yb)<sub>N</sub>(a)、Sr-10Y-Zr(b)和 Y/Yb-Sr/Y-La/Yb(c)判别图解

Fig.9 The discrimination diagrams of Sr/Y-(La/Yb)<sub>N</sub>(a), Sr-10Y-Zr (b) and Y/Yb-Sr/Y-La/Yb (c) for biotite granodiorites  
图a底图据 Liu et al.(2010);图b和c的底图据朱弟成等(2002)

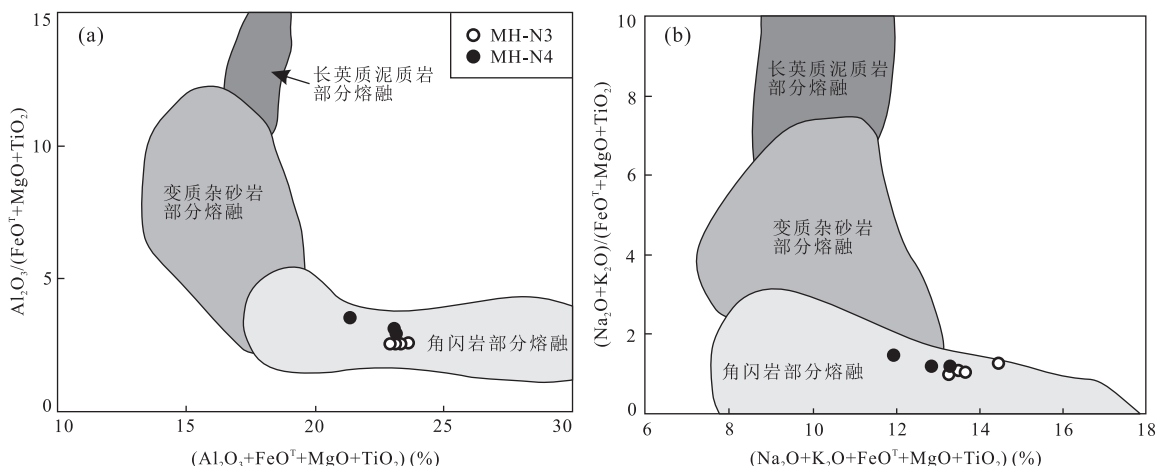


图10 黑云母花岗闪长岩源区判别图解

Fig.10 Discriminant diagrams of source regions for biotite granodiorites  
底图据 Patiño (1999)

指示其形成于高压环境(通常大于 1.5 GPa; Xiong et al., 2005),贫 Y 和 Yb 暗示源区可能残留石榴子石、角闪石等,而富 Sr、负 Eu 异常不明显则说明熔融时斜长石在源区是不稳定的,几乎全部进入岩浆。岩石中岩浆锆石  $\epsilon_{\text{Hf}}(t)$  值介于  $-3.26 \sim -1.46$ , 锆石 Hf 同位素成分变化范围较小,表明岩石源区均一定程度较高(图 7).结合其二阶段模式年龄( $t_{\text{DM2}} = 1.25 \sim 1.59$  Ga)和该时期的地幔特征(武广等,2005; Wu et al., 2011; Tang et al., 2014, 2016),笔者认为该岩石的岩浆可能起源于中元古代亏损地幔新增生的基性下地壳物质的部分熔融,而该岩石中锆石略负的  $\epsilon_{\text{Hf}}(t)$  值( $-3.26 \sim -1.46$ )则是 Hf 同位素演化的结果,而非其他地幔源区的特征。

#### 4.2 构造背景

如前所述,黑云母花岗闪长岩样品富硅、富铝、贫镁,具有弧岩浆岩的微量元素地球化学性质,富集

Ba、K、La、Ce 等大离子亲石元素,明显亏损 Nb、Ta、Ti 等高场强元素,具有明显的“TNT”效应(韦忠良等,2008; Chen et al., 2011; Tang et al., 2014).与典型岛弧岩浆岩相比,该岩石具有更低 HREE(尤其 Yb, 图 8)和更高的 Sr 含量,暗示两者在同一背景下具有不同深度的岩浆源区.岩石具有较低的 MgO、CaO 含量,  $\text{Na}_2\text{O}/\text{K}_2\text{O} > 1.17$ , 显示其具有活动大陆边缘环境火成岩特征(Gill, 1987; Fran-calanci et al., 1993).岩石属于 I 型花岗岩,  $\text{Al}_2\text{O}_3$  含量为  $16.58\% \sim 17.34\% (> 13\%)$ , CaO 含量为  $3.35\% \sim 3.97\% (> 1.73\%)$ ,  $\text{K}_2\text{O}$  含量为  $2.68\% \sim 3.39\% (< 4\%)$ ,  $(\text{Na}_2\text{O} + \text{K}_2\text{O})$  含量为  $6.67\% \sim 8.07\% (< 8\%)$ , 显示其形成于挤压的火山弧环境(邱家骥, 2004; 刘金龙等, 2015b).此外,结合岩体具有弧岩浆微量元素组合的特征且出现明显的 Nb、Ta、Ti 亏损,表明其成因与俯冲作用关系密切(董增产等,

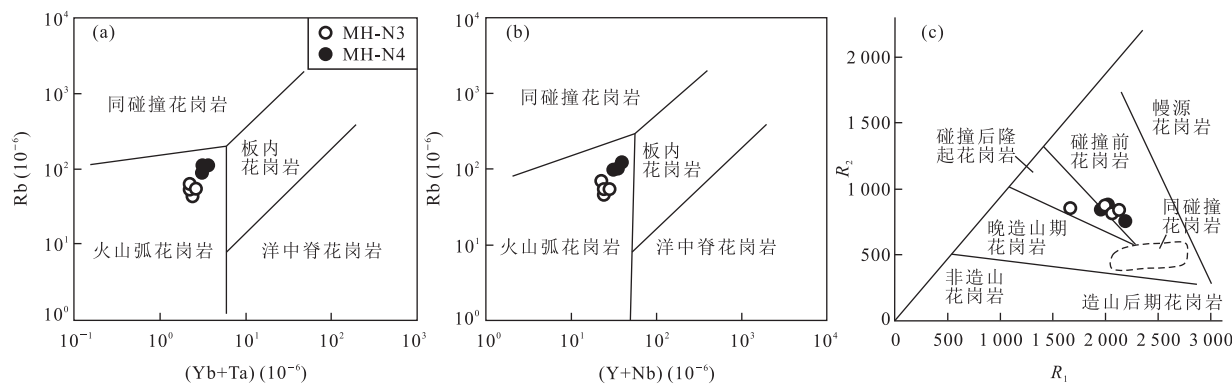


图 11 黑云母花岗闪长岩(Yb+Ta)-Rb(a)、(Y+Nb)-Rb(b) 和  $R_1$ - $R_2$ (c) 构造判别图解

Fig.11 Tectonic discrimination diagrams of (Yb+Ta)-Rb (a), (Y+Nb)-Rb (b) and  $R_1$ - $R_2$  (c) for biotite granodiorites  
 图 a 和 b 底图据 Pearce *et al.* (1984); 图 c 底图据 Batchelor and Bowden (1985)

2015).在图 11a 和 11b 中岩石均落入火山弧环境, 在图 11c 中样品落入板块碰撞前消减地区花岗岩的区域, 即活动大陆边缘环境。蒙古—鄂霍茨克洋形成于早二叠世(莫申国等, 2005), 早在晚古生代末期鄂霍茨克大洋板块就存在局部俯冲, 并持续到三叠纪(陈志广等, 2010; 许文良等, 2013; Tang *et al.*, 2014, 2016)。近年来越来越多的资料显示该大洋板块存在向南俯冲: 产于安第斯型大陆边缘环境的中蒙古 Hangayn 岩基(255~230 Ma; Tomurtogoo *et al.*, 2005; Orolmaa *et al.*, 2008), 蒙古国额尔登特地区发育的岛弧环境的侵入杂岩及与之相关的特大型斑岩型铜—钼矿床(240 Ma; 江思宏等, 2010), 额尔古纳一根河地区发现的一套具有活动陆缘构造背景的早侏罗世玄武岩—玄武安山岩钙碱性火山岩组合(Zhang *et al.*, 2008; 许文良等, 2013), 我国境内额尔古纳地块中的一系列形成于早中生代的斑岩型铜钼矿床(Macpherson *et al.*, 2006), 内蒙古满洲里地区的八大关杂岩形成于活动大陆边缘岛弧环境(203~214 Ma; 曾维顺等, 2014)。此外, Tang *et al.* (2014)研究认为内蒙古莫尔道嘎地区的早三叠世中酸性侵入岩形成于蒙古—鄂霍茨克洋向南俯冲的岛弧构造环境。蒙古—鄂霍茨克造山带南侧发育一条巨型的 NE 向中生代岩浆岩带, 岩石组合为闪长岩、石英闪长岩、花岗闪长岩、二长花岗岩、正长花岗岩等, 被认为其形成与蒙古—鄂霍茨克洋板块向南俯冲有关(Xu *et al.*, 2013; 许文良等, 2013; Tang *et al.*, 2014, 2016; Zhao *et al.*, 2016)。大兴安岭北部偏碱性的早中生代火山岩的广泛发育可能反映蒙古—鄂霍茨克洋向南俯冲的弧后伸展环境(李碧乐等, 2016)。漠河盆地的二十二站组碎屑岩为蒙古—鄂霍茨克洋闭合后南北两侧物源区被快速剥蚀、快

速搬运而沉积成岩的产物, 该大洋东段在晚侏罗世时期闭合(李良等, 2017)。由此可知, 漠河县城南的黑云母花岗闪长岩形成于蒙古—鄂霍茨克洋板块向南俯冲的活动大陆边缘环境。

研究表明, 西伯利亚板块相对于中蒙地块旋转的独特运动方式使得蒙古—鄂霍茨克洋发生自西向东剪刀式的闭合(Zhao *et al.*, 1990; Zorin, 1999; Parfenov *et al.*, 2001), 西部始于晚三叠世, 而东部则始于中—晚侏罗世(Zonenshain *et al.*, 1990; Zroin, 1999)并持续到晚侏罗世—早白垩世(Kravchinsky *et al.*, 2002)。黑龙江孙吴地区的中侏罗世白云母花岗岩的形成与蒙古—鄂霍茨克洋闭合过程中的陆—陆碰撞作用有关(李宇等, 2015), 表明此时蒙古—鄂霍茨克洋已经闭合。满洲里地区发现了晚侏罗世的火山岩组合(Zhang *et al.*, 2008; 孟恩等, 2011; 许文良等, 2013), 是与蒙古—鄂霍茨克造山带有关的加厚陆壳坍塌阶段或拆沉阶段的产物。中侏罗世时期, 从小兴安岭西北部至冀北—辽西地区发生了一次重要的陆壳加厚与逆冲推覆事件, 且其推覆方向与蒙古—鄂霍茨克洋的闭合有关(李宇等, 2015)。

#### 4.3 成矿意义

埃达克岩具有较强的成矿专属属性, 浅成低温热液 Au-Ag 及斑岩型 Cu-Cu-Au 矿床与埃达克岩具有密切的成因联系(Thieblemont *et al.*, 1997; Sajona and Maury, 1998), 我国多数斑岩型铜(金、钼)矿与埃达克岩密切相关(张旗等, 2004)。额尔古纳地块较多早中生代的花岗质岩石具有埃达克岩的特征, 其中不乏大型矿床, 如乌奴格吐山特大型 Cu-Mo 矿(177~204 Ma; 秦克章等, 1999)、太平川 Cu-Mo 矿(184~202 Ma; 陈志广等, 2010; 王召林等, 2010)和二十一站 Cu-Au 矿等斑岩型矿床。这些成矿斑岩体

均具有C型埃达克岩的特征,这说明了额尔古纳地块的早中生代C型埃达克岩具有较大的成矿潜力,不容忽视。张旗等(2009)指出埃达克岩分布区应为我国寻找斑岩型和低温热液型Au-Ag矿的重点区域,建议首先突破O型埃达克岩分布区,因为O型埃达克岩控制了全球大部分铜矿的产出,超大型和超巨型的斑岩型铜矿大多与板块俯冲作用相关;但也不能忽视C型埃达克岩,因为我国现有的大型和超大型Cu、Au和Mo矿床多与C型埃达克岩有关,包括德兴、玉龙、胶东、小秦岭和南泥湖等。早中生代时期,研究区处于蒙古—鄂霍茨克洋向南俯冲的活动大陆边缘环境(Xu et al., 2013;许文良等,2013; Tang et al., 2014, 2016; Zhao et al., 2016),岩浆侵入活动强烈,埃达克岩发育,应加强其含矿性评价和找矿工作。

## 5 结论

(1) 镔石LA-ICP-MS U-Pb测年获得漠河县城南的黑云母花岗闪长岩的加权平均年龄分别为 $185 \pm 2$  Ma和 $182 \pm 2$  Ma,属早侏罗世,代表区域上一期强烈的岩浆事件。

(2) 研究区黑云母花岗闪长岩属于高钾钙碱性埃达克岩类,具有高Sr低Y的特征和微弱的Eu负异常,其 $\epsilon_{\text{Hf}}(t)$ 值为 $-3.26 \sim -1.46$ ,对应的二阶段模式年龄为 $1.25 \sim 1.59$  Ga。该岩石的岩浆可能起源于中元古代亏损地幔新增生的基性下地壳物质的部分熔融。

(3) 岩石富硅、富钾、贫镁,富集大离子亲石元素和亏损高场强元素,形成于蒙古—鄂霍茨克洋板块向南俯冲的活动大陆边缘环境。

致谢: 镔石LA-ICP-MS U-Pb定年工作得到了西北大学大陆动力学国家重点实验室同仁的鼎力帮助,Hf同位素分析得到了天津地质矿产研究所同位素实验室的帮助,两位审稿专家对本文提出了诸多建设性的意见和建议,在此一并表示衷心的感谢。

## References

- Andersen, T., 2002. Correction of Common Lead in U-Pb Analyses that Do Not Report  $^{204}\text{Pb}$ . *Chemical Geology*, 192 (1–2): 59–79. [https://doi.org/10.1016/s0009-2541\(02\)00195-x](https://doi.org/10.1016/s0009-2541(02)00195-x)
- Atherton, M.P., Petford, N., 1993. Generation of Sodium-Rich Magmas from Newly Underplated Basaltic Crust. *Nature*, 362: 144–146. <https://doi.org/10.1038/362144a0>
- Batchelor, R. A., Bowden, P., 1985. Petrogenetic Interpretation of Granitoid Rock Series Using Multicationic Parameters. *Chemical Geology*, 48 (1–4): 43–55. [https://doi.org/10.1016/0009-2541\(85\)90034-8](https://doi.org/10.1016/0009-2541(85)90034-8)
- Boynton, W. V., 1984. Geochemistry of the Rare Earth Elements: Meteorite Studies. In: Henderson, P., ed., *Rare Earth Element Geochemistry*. Elsevier, Amsterdam.
- Bureau of Geology and Mineral Resources of Inner Mongolia Autonomous Region (BGMRI), 1991. *Regional Geology of Inner Mongolia Autonomous Region*. Geological Publishing House, Beijing (in Chinese).
- Bureau of Geology and Mineral Resources of Heilongjiang Province (BGMRH), 1993. *Regional Geology of Heilongjiang Province*. Geological Publishing House, Beijing (in Chinese).
- Castillo, P. R., Janney, P. E., Solidum, R. U., 1999. Petrology and Geochemistry of Camiguin Island, Southern Philippines: Insights to the Source of Adakites and Other Lavas in a Complex Arc Setting. *Contributions to Mineralogy and Petrology*, 134 (1): 33–51. <https://doi.org/10.1007/s004100050467>
- Chen, Z.G., Zhang, L.C., Lu, B.Z., et al., 2010. Geochronology and Geochemistry of the Taipingchuan Copper-Molybdenum Deposit in Inner Mongolia, and Its Geological Significances. *Acta Petrologica Sinica*, 26 (5): 1437–1449 (in Chinese with English abstract).
- Chen, Z.G., Zhang, L.C., Wan, B., et al., 2011. Geochronology and Geochemistry of the Wunugetushan Porphyry Cu-Mo Deposit in NE China, and Their Geological Significance. *Ore Geology Reviews*, 43: 92–105. <https://doi.org/10.1016/j.oregeorev.2011.08.007>
- Chu, N.C., Taylor, R.N., Chavagnac, V., et al., 2002. Hf Isotope Ratio Analysis Using Multi-Collector Inductively Coupled Plasma Mass Spectrometry: An Evaluation of Isobaric Interference Corrections. *Journal of Analytical Atomic Spectrometry*, 17 (12): 1567–1574. <https://doi.org/10.1039/b206707b>
- Defant, M. J., Drummond, M. S., 1990. Derivation of Some Modern Arc Magmas by Melting of Young Subducted Lithosphere. *Nature*, 347: 662–665. <https://doi.org/10.1038/347662a0>
- Ding, H.X., Hou, Q.Y., Zhang, Z.M., 2016. Petrogenesis and Tectonic Significance of the Eocene Adakite-Like Rocks in Western Yunnan, Southeastern Tibetan Plateau. *Lithos*, 245: 161–173. <https://doi.org/10.1016/j.lithos.2015.09.024>
- Dong, Z.C., Gu, P.Y., Chen, R.M., et al., 2015. Geochronology, Geochemistry, and Hf Isotope of Yanchangbeishan

- Adamellite of Lenghu Area in Qinghai. *Earth Science*, 40(1):130—144 (in Chinese with English abstract). <https://doi.org/10.3799/dqkx.2015.009>
- Francalanci, L., Taylor, S. R., McCulloch, M. T., et al., 1993. Geochemical and Isotopic Variations in the Calc-Alkaline Rocks of Aeolian Arc, Southern Tyrrhenian Sea, Italy: Constraints on Magma Genesis. *Contributions to Mineralogy and Petrology*, 113(3): 300—313. <https://doi.org/10.1007/bf00286923>
- Gao, S., Jin, Z. M., 1997. Delamination and Its Geodynamical Significance for the Crust-Mantle Evolution. *Geological Science and Technology Information*, 16(1): 1—8 (in Chinese with English abstract).
- Gao, S., Rudnick, R. L., Yuan, H. L., et al., 2004. Recycling Lower Continental Crust in the North China Craton. *Nature*, 432: 892—897. <https://doi.org/10.1038/nature03162>
- Geng, J.Z., Li, H.K., Zhang, J., et al., 2011. Zircon Hf Isotope Analysis by Means of LA-MC-ICP-MS. *Geological Bulletin of China*, 30(10): 1508—1513 (in Chinese with English abstract).
- Gill, J. B., 1987. Early Geochemical Evolution of an Oceanic Island Arc and Back Arc: Fiji and the South Fiji Basin. *The Journal of Geology*, 95(5): 589—615.
- Gou, J., Sun, D. Y., Ren, Y. S., et al., 2013. Petrogenesis and Geodynamic Setting of Neoproterozoic and Late Paleozoic Magmatism in the Manzhouli-Erguna Area of Inner Mongolia, China: Geochronological, Geochemical and Hf Isotopic Evidence. *Journal of Asian Earth Sciences*, 67—68: 114—137. <https://doi.org/10.1016/j.jseaes.2013.02.016>
- Griffin, W. L., Wang, X., Jackson, S. E., et al., 2002. Zircon Chemistry and Magma Mixing, SE China: In-Situ Analysis of Hf Isotope, Tonglu and Pingtan Igneous Complexes. *Lithos*, 61(3—4): 237—269. [https://doi.org/10.1016/s0024-4937\(02\)00082-8](https://doi.org/10.1016/s0024-4937(02)00082-8)
- Hou, H. X., Zhang, D. H., Zhang, R. Z., 2016. The Chronology, Geochemical Characteristics and Geological Significance of the Mesozoic Shiyagou Hidden Granite at the East Qinling. *Earth Science*, 41(10): 1665—1682 (in Chinese with English abstract). <https://doi.org/10.3799/dqkx.2016.122>
- Jiang, S. H., Nie, F. J., Su, Y. J., et al., 2010. Geochronology and Origin of the Erdenet Superlarge Cu-Mo Deposit in Mongolia. *Acta Geoscientia Sinica*, 31(3): 289—306 (in Chinese with English abstract).
- Kay, S. M., Mpodozis, C., 2001. Central Andean Ore Deposits Linked to Evolving Shallow Subduction Systems and Thickening Crust. *GSA Today*, 11(3): 4—9. [https://doi.org/10.1130/1052-5173\(2001\)011<0004:caodlt>2.0.co;2](https://doi.org/10.1130/1052-5173(2001)011<0004:caodlt>2.0.co;2)
- Kravchinsky, V.A., Cogné, J.P., Harbert, W.P., et al., 2002. Evolution of the Mongol-Okhotsk Ocean as Constrained by New Palaeomagnetic Data from the Mongol-Okhotsk Suture Zone, Siberia. *Geophysical Journal International*, 148(1): 34—57. <https://doi.org/10.1046/j.1365-246x.2002.01557.x>
- Lai, S.C., Liu, C.Y., Yi, H.S., 2003. Geochemistry and Petrogenesis of Cenozoic Andesite-Dacite Associations from the Hoh Xil Region, Tibetan Plateau. *International Geology Review*, 45(11): 998—1019. <https://doi.org/10.2747/0020-6814.45.11.998>
- Li, B.L., Sun, Y.G., Chen, G.J., et al., 2016. Zircon U-Pb Geochronology, Geochemistry and Hf Isotopic Composition and Its Geological Implication of the Fine-Grained Syenogranite in Dong'an Goldfield from the Lesser Xing'an Mountains. *Earth Science*, 41(1): 1—16 (in Chinese with English abstract). <https://doi.org/10.3799/dqkx.2016.001>
- Li, J. Y., He, Z. J., Mo, S. G., et al., 2004a. The Age of Conglomerates in the Lower Part of the Xiufeng Formation in the Northern Da Hinggan Mountains, NE China, and Their Tectonic Implications. *Geological Bulletin of China*, 23(2): 120—129 (in Chinese with English abstract).
- Li, J. Y., Mo, S. G., He, Z. J., et al., 2004b. The Timing of Crustal Sinistral Strike-Slip Movement in the Northern Great Khing'an Ranges and Its Constraint on Reconstruction of the Crustal Tectonic Evolution of NE China and Adjacent Areas since the Mesozoic. *Earth Science Frontiers*, 11(3): 157—167 (in Chinese with English abstract).
- Li, J. Y., Zhang, J., Yang, T. N., et al., 2009. Crustal Tectonic Division and Evolution of the Southern Part of the North Asian Orogenic Region and Its Adjacent Areas. *Journal of Jilin University (Earth Science Edition)*, 39(4): 584—605 (in Chinese with English abstract).
- Li, L., Sun, F. Y., Li, B. L., et al., 2015. Ore-Forming Fluid Features and Genesis of Shabaosi Gold Deposit in Mohe County, Heilongjiang Province. *Earth Science*, 40(7): 1163—1176 (in Chinese with English abstract). <https://doi.org/10.3799/dqkx.2015.097>
- Li, L., Sun, F. Y., Li, B. L., et al., 2017. Geochronology of Ershi'erzhan Formation Sandstone in Mohe Basin and Tectonic Environment of Its Provenance. *Earth Science*, 42(1): 35—52 (in Chinese with English abstract). <https://doi.org/10.3799/dqkx.2017.003>
- Li, Y., Ding, L. L., Xu, W. L., et al., 2015. Geochronology and Geochemistry of Muscovite Granites in Sunwu Area, NE China: Implications for the Timing of Closure of the

- Mongol-Okhotsk Ocean. *Acta Petrologica Sinica*, 31(1):56—66 (in Chinese with English abstract).
- Liu, J.L., Sun, F.Y., Li, L., et al., 2015a. Geochronology, Geochemistry and Hf Isotopes of Gerizhuotuo Complex Intrusion in West of Anyemaqen Suture Zone. *Earth Science*, 40(6): 965—981 (in Chinese with English abstract). <https://doi.org/10.3799/dqkx.2015.081>
- Liu, J.L., Sun, F. Y., Lin, B. L., 2015b. Geochronology, Geochemistry and Zircon Hf Isotope of Miantian Granodiorite Intrusion in Yanbian Region, Southern Jilin Province and Its Geological Significance. *Earth Science*, 40(1):49—60 (in Chinese with English abstract). <https://doi.org/10.3799/dqkx.2015.004>
- Liu, J.L., Sun, F. Y., Zhang, Y.J., et al., 2016. Zircon U-Pb Geochronology, Geochemistry and Hf Isotopes of Nankouqian Granitic Intrusion in Qingyuan Region, Liaoning Province. *Earth Science*, 41(1):55—66 (in Chinese with English abstract). <https://doi.org/10.3799/dqkx.2016.004>
- Liu, S.A., Li, S.G., He, Y.S., et al., 2010. Geochemical Contrasts between Early Cretaceous Ore-Bearing and Ore-Barren High-Mg Adakites in Central-Eastern China: Implications for Petrogenesis and Cu-Au Mineralization. *Geochimica et Cosmochimica Acta*, 74(24): 7160—7178. <https://doi.org/10.1016/j.gca.2010.09.003>
- Ludwig, K.R., 2003. User's Manual for Isoplot 3.00: A Geochronological Toolkit for Microsoft Excel. Berkeley Geochronology Center Special Publication, Berkeley.
- Macpherson, C.G., Dreher, S.T., Thirlwall, M.F., 2006. Adakites Without Slab Melting: High Pressure Differentiation of Island Arc Magma, Mindanao, the Philippines. *Earth and Planetary Science Letters*, 243(3—4), 581—593.
- Maniar, P.D., Piccoli, P.M., 1989. Tectonic Discrimination of Granitoids. *Geological Society of America Bulletin*, 101(5): 635—643. [https://doi.org/10.1130/0016-7606\(1989\)101<0635:tdog>2.3.co;2](https://doi.org/10.1130/0016-7606(1989)101<0635:tdog>2.3.co;2)
- Martin, H., 1999. Adakitic Magmas: Modern Analogues of Archaean Granitoids. *Lithos*, 46(3): 411—429. [https://doi.org/10.1016/s0024-4937\(98\)00076-0](https://doi.org/10.1016/s0024-4937(98)00076-0)
- McKenzie, D., 1989. Some Remarks on the Movement of Small Melt Fractions in the Mantle. *Earth and Planetary Science Letters*, 95(1—2): 53—72. [https://doi.org/10.1016/0012-821X\(89\)90167-2](https://doi.org/10.1016/0012-821X(89)90167-2)
- Meng, E., Xu, W. L., Yang, D. B., et al., 2011. Zircon U-Pb Chronology, Geochemistry of Mesozoic Volcanic Rocks from the Lingquan Basin in Manzhouli Area, and Its Tectonic Implications. *Acta Petrologica Sinica*, 27(4): 1209—1226 (in Chinese with English abstract).
- Mo, S.G., Han, M.L., Li, J.Y., 2005. Compositions and Orogenic Processes of Mongolia-Okhotsk Orogen. *Journal of Shandong University of Science and Technology (Natural Science)*, 24(3): 50—52 (in Chinese with English abstract).
- Orolmaa, D., Erdenesaihan, G., Borisenko, A. S., et al., 2008. Permian-Triassic Granitoid Magmatism and Metallogeny of the Hangayn (central Mongolia). *Russian Geology and Geophysics*, 49(7): 534—544. <https://doi.org/10.1016/j.rgg.2008.06.008>
- Oyarzun, R., Márquez, A., Lillo, J., et al., 2001. Giant Versus Small Porphyry Copper Deposits of Cenozoic Age in Northern Chile: Adakitic Versus Normal Calc-Alkaline Magmatism. *Mineralium Deposita*, 36(8): 794—798. <https://doi.org/10.1007/s001260100205>
- Parfenov, L. M., Popeko, L. I., Tomurtogoo, O., 2001. Problems of Tectonics of the Mongolia-Okhotsk Orogenic Belt. *Geology of the Pacific Ocean*, 16(5): 797—830.
- Patchett, P. J., Tatsumoto, M., 1980. A Routine High-Precision Method for Lu-Hf Isotope Geochemistry and Chronology. *Contributions to Mineralogy and Petrology*, 75(3): 263—267. <https://doi.org/10.1007/bf01166766>
- Patino, D. A. E., 1999. What do Experiments Tell Us about the Relative Contributions of Crust and Mantle to the Origin of Granitic Magmas? In: Castro, A., Fernandez, C., Vigneresse, J. L., eds., Understanding Granites: Integrating New and Classical Techniques. *Geological Society, London, Special Publication*, 168: 55—75.
- Pearce, J. A., Harris, N. B. W., Tindle, A. G., 1984. Trace Element Discrimination Diagrams for the Tectonic Interpretation of Granitic Rocks. *Journal of Petrology*, 25(4): 956—983. <https://doi.org/10.1093/petrology/25.4.956>
- Peccerillo, A., Taylor, S. R., 1976. Geochemistry of Eocene Calc-Alkaline Volcanic Rocks from the Kastamonu Area, Northern Turkey. *Contributions to Mineralogy and Petrology*, 58(1): 63—81. <https://doi.org/10.1007/bf00384745>
- Qin, K.Z., Li, H.M., Li, W.S., et al., 1999. Intrusion and Mineralization Ages of the Wunugetushan Porphyry Cu-Mo Deposit, Inner Mongolia, Northwestern China. *Geological Review*, 45(2): 180—185 (in Chinese with English abstract).
- Qin, X. F., Yin, Z. G., Wang, Y., et al., 2007. Early Paleozoic Adakitic Rocks in Mohe Area at the Northern End of the Da Hinggan Mountains and Their Geological Significance. *Acta Petrologica Sinica*, 23(6): 1501—1511 (in Chinese with English abstract). <https://doi.org/10.3969/j.issn.1000-0569.2007.06.024>

- Qiu, J. X., 2004. Opening-Closing Tectonics and Magmatic Activity. *Geological Bulletin of China*, 23 (3): 222—231 (in Chinese with English abstract). <https://doi.org/10.3969/j.issn.1671-2552.2004.03.008>
- Rabbia, O. M., Correa, K. J., Hernández, L. B., et al., 2017. “Normal” to Adakite-Like Arc Magmatism Associated with the El Abra Porphyry Copper Deposit, Central Andes, Northern Chile. *International Journal of Earth Sciences*, 106 (8): 2687 — 2711. <https://doi.org/10.1007/s00531-017-1454-0>
- Rapp, R.P., Watson, E.B., 1995. Dehydration Melting of Metabasalt at 8 — 32 Kbar: Implications for Continental Growth and Crust-Mantle Recycling. *Journal of Petrology*, 36(4): 891—931. <https://doi.org/10.1093/petrology/36.4.891>
- Richards, J.P., Kerrich, R., 2007. Special Paper: Adakite-Like Rocks: Their Diverse Origins and Questionable Role in Metallogenesis. *Economic Geology*, 102 (4): 537 — 576. <https://doi.org/10.2113/gsecongeo.102.4.537>
- Sajona, F.G., Maury, R.C., 1998. Association of Adakites with Gold and Copper Mineralization in the Philippines. *Comptes Rendus de l'Académie des Sciences-Series-IIA-Earth and Planetary Science*, 326(1): 27 — 34. [https://doi.org/10.1016/s1251-8050\(97\)83200-4](https://doi.org/10.1016/s1251-8050(97)83200-4)
- Stern, C.R., Kilian, R., 1996. Role of the Subducted Slab, Mantle Wedge and Continental Crust in the Generation of Adakites from the Andean Austral Volcanic Zone. *Contributions to Mineralogy and Petrology*, 123: 263—281.
- Streckeisen, A. L., 1976. Classification of the Common Igneous Rocks by Means of Their Chemical Composition: A Provisional Attempt. *Neues Jahrbuch für Mineralogie-Monatshefte*, 1: 1—15.
- Sun, S. S., McDonough, W. F., 1989. Chemical and Isotopic Systematics of Oceanic Basalts: Implications for Mantle Composition and Processes. In; Saunders, A. D., Norry, M.J., eds., Magmatism in Ocean Basins. *Geological Society, London, Special Publications*, 42(1): 313—345. <https://doi.org/10.1144/gsl.sp.1989.042.01.19>
- Tang, J., Xu, W.L., Wang, F., et al., 2014. Geochronology and Geochemistry of Early-Middle Triassic Magmatism in the Erguna Massif, NE China: Constraints on the Tectonic Evolution of the Mongol-Okhotsk Ocean. *Lithos*, 184 — 187: 1 — 16. <https://doi.org/10.1016/j.lithos.2013.10.024>
- Tang, J., Xu, W. L., Wang, F., et al., 2016. Early Mesozoic Southward Subduction History of the Mongol-Okhotsk Oceanic Plate: Evidence from Geochronology and Geochemistry of Early Mesozoic Intrusive Rocks in the Erguna Massif, NE China. *Gondwana Research*, 31: 218 — 240. <https://doi.org/10.1016/j.gr.2014.12.010>
- Thiéblemont, D., Stein, G., Lescuyer, J. L., 1997. Gisements Épithermaux et Porphyriques: La Connexion Adakite. *Comptes Rendus de l'Académie des Sciences-Series-IIA-Earth and Planetary Science*, 325 (2): 103 — 109. [https://doi.org/10.1016/s1251-8050\(97\)83970-5](https://doi.org/10.1016/s1251-8050(97)83970-5)
- Tomurtogoo, O., Windley, B. F., Kroner, A., et al., 2005. Zircon Age and Occurrence of the Adaatsag Ophiolite and Muron Shear Zone, Central Mongolia: Constraints on the Evolution of the Mongol-Okhotsk Ocean, Suture and Orogen. *Journal of the Geological Society*, 162 (1): 125 — 134. <https://doi.org/10.1144/0016-764903-146>
- Wang, Q., Zhao, Z. H., Bai, Z. H., et al., 2003a. Carboniferous Adakites and Nb-Enriched Arc Basaltic Rocks Association in the Alataw Mountains, North Xinjiang: Interactions between Slab Melt and Mantle Peridotite and Implications for Crustal Growth. *Chinese Science Bulletin*, 48 (19): 2108 — 2115. <https://doi.org/10.1007/bf03037015>
- Wang, Q., Zhao, Z. H., Xu, J. F., et al., 2003b. Petrogenesis and Metallogenesis of the Yanshanian Adakite-Like Rocks in the Eastern Yangtze Block. *Science China Earth Sciences*, 46(Supp.): 164 — 176.
- Wang, Q., Zhao, Z. H., Xu, J. F., et al., 2006. Carboniferous Adakite-High-Mg Andesite-Nb-Enriched Basaltic Rock Suites in the Northern Tianshan Area: Implications for Phanerozoic Crustal Growth in the Central Asia Orogenic Belt and Cu-Au Mineralization. *Acta Petrologica Sinica*, 22 (1): 11—30 (in Chinese with English abstract).
- Wang, Z. L., Jin, J., Li, Z. L., et al., 2010. Zircon U-Pb Ages and Hf Isotopic Characteristics of Mineralized Porphyries in the Mordaoga Area, Northern-Central Da Hinggan Mountains, and Their Metallogenic Significance. *Acta Petrologica et Mineralogica*, 29 (6): 796 — 810 (in Chinese with English abstract).
- Wei, Z. L., Zhang, H., Guo, W. M., et al., 2008. LA-ICP-MS Zircon U-Pb Dating: Constraints on Late Mesozoic Regional Unconformity Timing in the Northern Hebei-Western Liaoning Provinces. *Progress in Natural Science*, 18(10): 1119—1127 (in Chinese ).
- Weng, W.F., Zhi, L.G., Cai, L. Y., et al., 2011. Geochemical Characteristics and Petrogenesis of the Mesozoic Adakite in South Anhui Province. *Geological Survey and Research*, 34 (2): 98—107 (in Chinese with English abstract).
- Wu, F.Y., Sun, D.Y., Ge, W.C., et al., 2011. Geochronology of the Phanerozoic Granitoids in Northeastern China. *Jour-*

- nal of Asian Earth Sciences*, 41(1): 1–30. <https://doi.org/10.1016/j.jseas.2010.11.014>
- Wu, F.Y., Zhao, G.C., Sun, D.Y., 2007. The Hulan Group: Its Role in the Evolution of the Central Asian Orogenic Belt of NE China. *Journal of Asian Earth Sciences*, 30 (3–4): 542–556. <https://doi.org/10.1016/j.jseas.2007.01.003>
- Wu, G., Chen, Y.C., Chen, Y.J., et al., 2012. Zircon U-Pb Ages of the Metamorphic Supracrustal Rocks of the Xinghuadukou Group and Granitic Complexes in the Argun Massif of the Northern Great Hinggan Range, NE China, and Their Tectonic Implications. *Journal of Asian Earth Sciences*, 49: 214–233. <https://doi.org/10.1016/j.jseas.2011.11.023>
- Wu, G., Chen, Y.J., Sun, F.Y., et al., 2008. Geochemistry of the Late Jurassic Granitoids in the Northern End Area of Da Hinggan Mountains and Their Geological and Prospecting Implications. *Acta Petrologica Sinica*, 24 (4): 899–910 (in Chinese with English abstract).
- Wu, G., Sun, F.Y., Zhao, C.S., et al., 2005. Discovery of the Early Paleozoic Post-Collisional Granites in Northern Margin of Erguna Massif and Its Geological Significance. *Chinese Science Bulletin*, 50(20): 2278–2288 (in Chinese).
- Wu, G., Sun, F.Y., Zhao, C.S., et al., 2007. Fluid Inclusion Study on Gold Deposits in Northwestern Erguna Metallogenic Belt, China. *Acta Petrologica Sinica*, 23 (9): 2227–2240 (in Chinese with English abstract).
- Xiao, L., Clemens, J.D., 2007. Origin of Potassic (C-Type) Adakite Magmas: Experimental and Field Constraints. *Lithos*, 95(3–4): 399–414. <https://doi.org/10.1016/j.lithos.2006.09.002>
- Xiong, X.L., Adam, J., Green, T.H., et al., 2005. Trace Element Characteristics of Partial Melts Produced by Melting of Metabasalts at High Pressures: Constraints on the Formation Condition of Adakitic Melts. *Science China Earth Sciences*, 49 (9): 915–925. <https://doi.org/10.1007/s11430-006-0915-2>
- Xiong, X.L., Li, X.H., Xu, J.F., et al., 2003. Extremely High Na Adakite-Like Magmas Derived from Lower Crust Basaltic Underplate: the Zhantang Andesitic Rocks from Huchang Basin, SE China. *Geochemical Journal*, 37: 233–252. <https://doi.org/10.2343/geochemj.37.233>
- Xu, W.L., Pei, F.P., Wang, F., et al., 2013. Spatial-Temporal Relationships of Mesozoic Volcanic Rocks in NE China: Constraints on Tectonic Overprinting and Transformations between Multiple Tectonic Regimes. *Journal of Asian Earth Sciences*, 74: 167–193. <https://doi.org/10.1016/j.jseas.2013.04.003>
- Xu, W.L., Wang, F., Pei, F.P., et al., 2013. Mesozoic Tectonic Regimes and Regional Ore-Forming Background in NE China: Constraints from Spatial and Temporal Variations of Mesozoic Volcanic Rock Associations. *Acta Petrologica Sinica*, 29(2): 339–353 (in Chinese with English abstract).
- Yang, J.H., Wu, F.Y., Shao, J.A., et al., 2006. Constraints on the Timing of Uplift of the Yanshan Fold and Thrust Belt, North China. *Earth and Planetary Science Letters*, 246 (3–4): 336–352. <https://doi.org/10.1016/j.epsl.2006.04.029>
- Yuan, H.L., Gao, S., Liu, X.M., et al., 2004. Accurate U-Pb Age and Trace Element Determinations of Zircon by Laser Ablation-Inductively Coupled Plasma-Mass Spectrometry. *Geostandards and Geoanalytical Research*, 28 (3): 353–370. <https://doi.org/10.1111/j.1751-908x.2004.tb00755.x>
- Zeng, W.S., Zhou, J.B., Dong, C., et al., 2014. Subduction Record of Mongol-Okhotsk Ocean: Constraints from Badaguan Metamorphic Complexes in the Erguna Massif, NE China. *Acta Petrologica Sinica*, 30(7): 1948–1960 (in Chinese with English abstract).
- Zhang, J.F., Li, Z.T., Jin, C.Z., 2004. Adakites in Northeastern China and Their Mineralized Implications. *Acta Petrologica Sinica*, 20 (2): 361–368 (in Chinese with English abstract).
- Zhang, J.H., Ge, W.C., Wu, F.Y., et al., 2008. Large-Scale Early Cretaceous Volcanic Events in the Northern Great Xing'an Range, Northeastern China. *Lithos*, 102(1–2): 138–157. <https://doi.org/10.1016/j.lithos.2007.08.011>
- Zhang, Q., Wang, Y., Qian, Q., et al., 2001. The Characteristics and Tectonic-Metallogenetic Significances of the Adakites in Yanshan Period from Eastern China. *Acta Petrologica Sinica*, 17 (2): 236–244 (in Chinese with English abstract).
- Zhang, Q., Xu, J.F., Wang, Y., et al., 2004. Diversity of Adakite. *Geological Bulletin of China*, 23 (9–10): 959–965 (in Chinese with English abstract).
- Zhang, Q., Yin, X.M., Yin, Y., et al., 2009. Issues on Metallogenesis and Prospecting of Gold and Copper Deposits Related to Adakite and Himalayan Type Granite in West Qinling. *Acta Petrologica Sinica*, 25(12): 3103–3122 (in Chinese with English abstract).
- Zhao, S., Xu, W.L., Tang, J., et al., 2016. Timing of Formation and Tectonic Nature of the Purportedly Neoproterozoic Jiageda Formation of the Erguna Massif, NE China: Constraints from Field Geology and U-Pb Geo-

- chronology of Detrital and Magmatic Zircons. *Precambrian Research*, 281: 585—601. <https://doi.org/10.1016/j.precamres.2016.06.014>
- Zhao, X., Coe, R.S., Zhou, Y.X., et al., 1990. New Paleomagnetic Results from Northern China: Collision and Suturing with Siberia and Kazakhstan. *Tectonophysics*, 181 (1—4): 43—81. [https://doi.org/10.1016/0040-1951\(90\)90008-v](https://doi.org/10.1016/0040-1951(90)90008-v)
- Zhu, D.C., Duan, L.P., Liao, Z.L., et al., 2002. Discrimination for Two Kinds of Adakites. *Journal of Mineralogy and Petrology*, 22(3): 5—9 (in Chinese with English abstract).
- Zonenshain, L.P., Kuzmin, M.I., Natapov, L.M., et al., 1990. *Geology of the USSR: A Plate-Tectonic Synthesis*. American Geophysical union, Washington, D.C..
- Zorin, Y.A., 1999. Geodynamics of the Western Part of the Mongolia-Okhotsk Collisional Belt, Trans-Baikal Region (Russia) and Mongolia. *Tectonophysics*, 306 (1): 33—56. [https://doi.org/10.1016/s0040-1951\(99\)00042-6](https://doi.org/10.1016/s0040-1951(99)00042-6)
- ### 附中文参考文献
- 陈志广,张连昌,卢百志,等,2010.内蒙古太平川铜钼矿成矿斑岩时代、地球化学及地质意义.岩石学报,26(5): 1437—1449.
- 董增产,辜平阳,陈锐明,等,2015.柴北缘西端盐场北山二长花岗岩年代学、地球化学及其 Hf 同位素特征.地球科学,40(1): 130—144. doi: 10.3799/dqkx.2015.009
- 高山,金振民,1997.拆沉作用(delamination)及其壳—幔演化动力学意义.地质科技情报,16(1): 1—9.
- 耿建珍,李怀坤,张健,等,2011.锆石 Hf 同位素组成的 LA-MC-ICP-MS 测定.地质通报,30(10): 1508—1513. doi: 10.3969/j.issn.1671-2552.2011.10.004
- 黑龙江省地质矿产局,1993.黑龙江省区域地质志.北京:地质出版社.
- 侯红星,张德会,张荣臻,2016.东秦岭中生代石瑶沟隐伏花岗岩年代学、地球化学特征及地质意义.地球科学,41 (10): 1665—1682. doi: 10.3799/dqkx.2016.122
- 江思宏,聂凤军,苏永江,等,2010.蒙古国额尔登特特大型铜—钼矿床年代学与成因研究.地球学报,31(3): 289—306.
- 李碧乐,孙永刚,陈广俊,等,2016.小兴安岭东安金矿区细粒正长花岗岩 U-Pb 年龄、岩石地球化学、Hf 同位素组成及地质意义.地球科学,41(1): 1—16. doi: 10.3799/dqkx.2016.001
- 李锦轶,和政军,莫申国,等,2004a.大兴安岭北部绣峰组下部砾岩的形成时代及其大地构造意义.地质通报,23 (2): 120—129.
- 李锦轶,莫申国,何政军,等,2004b.大兴安岭北段地壳左行走滑运动的时代及其对中国东北及邻区中生代以来地壳构造演化重建的制约.地学前缘,11(3): 157—168.
- 李锦轶,张进,杨天南,等,2009.北亚造山区南部及其毗邻地区地壳构造分区与构造演化.吉林大学学报(地球科学版),39(4): 584—605.
- 李良,孙丰月,李碧乐,等,2015.黑龙江省漠河县砂宝斯金矿床流体特征及矿床成因.地球科学,40(7): 1163—1176. doi: 10.3799/dqkx.2015.097
- 李良,孙丰月,李碧乐,等,2017.漠河盆地二十二站组砂岩形成时代及物源区构造环境判别.地球科学,42(1): 35—52. doi: 10.3799/dqkx.2017.003
- 李宇,丁磊磊,许文良,等,2015.孙吴地区侏罗世白云母花岗岩的年代学与地球化学:对蒙古—鄂霍茨克洋闭合时间的限定.岩石学报,31(1): 56—66.
- 刘金龙,孙丰月,李良,等,2015a.青海阿尼玛卿蛇绿混杂岩带西段哥日卓托杂岩体年代学、地球化学及 Hf 同位素.地球科学,40(6): 965—981. doi: 10.3799/dqkx.2015.081
- 刘金龙,孙丰月,林博磊,等,2015b.吉林延边地区棉田岩体锆石 U-Pb 年代学、地球化学及 Hf 同位素.地球科学,40(1): 49—60. doi: 10.3799/dqkx.2015.004
- 刘金龙,孙丰月,张雅静,等,2016.辽宁省清原县南口前岩体锆石 U-Pb 年代学、地球化学及 Hf 同位素.地球科学,41(1): 55—66. doi: 10.3799/dqkx.2016.004
- 孟恩,许文良,杨德彬,等,2011.满洲里地区灵泉盆地中生代火山岩的锆石 U-Pb 年代学、地球化学及其地质意义.岩石学报,27(4): 1209—1226.
- 莫申国,韩美莲,李锦轶,2005.蒙古—鄂霍茨克造山带的组成及造山过程.山东科技大学学报(自然科学版),24 (3): 50—52.
- 内蒙古自治区地质矿产局,1991.内蒙古自治区区域地质志.北京:地质出版社.
- 秦克章,李惠民,李伟实,等,1999.内蒙古乌奴格吐山斑岩铜钼矿床的成岩、成矿时代.地质论评,45(2): 180—185.
- 秦秀峰,尹志刚,汪岩,等,2007.大兴安岭北端漠河地区早古生代埃达克质岩特征及地质意义.岩石学报,23(6): 1501—1511.
- 邱家骥,2004.开合构造与岩浆活动.地质通报,23(3): 222—231.
- 王强,赵振华,许继峰,等,2006.天山北部石炭纪埃达克岩—高镁安山岩—富 Nb 岛弧玄武质岩:对中亚造山带显生宙地壳增生与铜金成矿的意义.岩石学报,22(1): 11—30.
- 王召林,金浚,李占龙,等,2010.大兴安岭中北段莫尔道嘎地区含矿斑岩的锆石 U-Pb 年龄、Hf 同位素特征及成矿意义.岩石矿物学杂志,29(6): 796—810.
- 韦忠良,张宏,郭文敏,等,2008. LA-ICP-MS 锆石 U-Pb 测年对辽西—冀北地区晚中生代区域性角度不整合时代的约束.自然科学进展,18(10): 1119—1127.
- 翁望飞,支利庚,蔡连友,等,2011.皖南中生代高钾钙碱性埃

- 达克岩地球化学特征及岩石成因.地质调查与研究,34(2):98—107.
- 武广,孙丰月,赵财胜,等,2005.额尔古纳地块北缘早古生代后碰撞花岗岩的发现及其地质意义.科学通报,50(20):2278—2288.
- 武广,孙丰月,赵财胜,等,2007.额尔古纳成矿带西北部金矿床流体包裹体研究.岩石学报,23(9):2227—2240.
- 武广,陈衍景,孙丰月,等,2008.大兴安岭北端晚侏罗世花岗岩类地球化学及其地质和找矿意义.岩石学报,24(4):899—910.
- 许文良,王枫,裴福萍,等,2013.中国东北中生代构造体制与区域成矿背景:来自中生代火山岩组合时空变化的制约.岩石学报,29(2):339—353.
- 曾维顺,周建波,董策,等,2014.蒙古—鄂霍茨克洋俯冲的记  
录:额尔古纳地区八大关变质杂岩的证据.岩石学报,30(7):1948—1960.
- 张炯飞,李之彤,金成洙,2004.中国东北部地区埃达克岩及其成矿意义.岩石学报,20(2):361—368.
- 张旗,王焰,钱青,等,2001.中国东部燕山期埃达克岩的特征及其构造—成矿意义.岩石学报,17(2):236—244.
- 张旗,许继峰,王焰,等,2004.埃达克岩的多样性.地质通报,23(9—10):959—965.
- 张旗,殷先明,殷勇,等,2009.西秦岭与埃达克岩和喜马拉雅型花岗岩有关的金铜成矿及找矿问题.岩石学报,25(12):3103—3122.
- 朱弟成,段丽萍,廖忠礼,等,2002.两类埃达克岩的判别.矿物岩石,22(3):5—9.